creative commons
COMMONS DEED

저작자표시-비영리-변경금지 2.0 대한민국

이용자는 아래의 조건을 따르는 경우에 한하여 자유롭게

- 이 저작물을 복제, 배포, 전송, 전시, 공연 및 방송할 수 있습니다.

다음과 같은 조건을 따라야 합니다:

저작자표시. 귀하는 원저작자를 표시하여야 합니다.

비영리. 귀하는 이 저작물을 영리 목적으로 이용할 수 없습니다.

변경금지. 귀하는 이 저작물을 개작, 변형 또는 가공할 수 없습니다.

- 귀하는, 이 저작물의 재이용이나 배포의 경우, 이 저작물에 적용된 이용허락조건을 명확하게 나타내어야 합니다.
- 저작권자로부터 별도의 허가를 받으면 이러한 조건들은 적용되지 않습니다.

저작권법에 따른 이용자의 권리는 위의 내용에 의하여 영향을 받지 않습니다.

이것은 이용허락규약(Legal Code)을 이해하기 쉽게 요약한 것입니다.

Disclaimer

dCollection

연세대학교
YONSEI UNIVERSITY

Development and Validation of a Novel Neuro-Behavioral Subclassification System for Autism Spectrum Disorder

Chanyoung Ko

The Graduate School
Yonsei University
Department of Medicine

연세대학교
YONSEI UNIVERSITY

Development and Validation of a Novel Neuro-Behavioral Subclassification System for Autism Spectrum Disorder

A Dissertation Submitted
to the Department of Medicine
and the Graduate School of Yonsei University
in partial fulfillment of the
requirements for the degree of
Doctor of Philosophy in Medical Science

Chanyoung Ko

December 2024

연세대학교
YONSEI UNIVERSITY

This certifies that the Dissertation of Chanyoung Ko is approved.

Thesis Supervisor	Yu Rang Park
Thesis Committee Member	Jae-Jin Kim
Thesis Committee Member	Dukyong Yoon
Thesis Committee Member	Younghee Lee
Thesis Committee Member	JeongGil Ko

The Graduate School
Yonsei University
December 2024

연세대학교
YONSEI UNIVERSITY

ACKNOWLEDGEMENTS

Embarking on this PhD has been an extraordinary journey, and I am profoundly thankful for the widespread support and encouragement I have been fortunate to receive.

My deepest gratitude goes to my advisor, Dr. Yu Rang Park, whose mentorship has been invaluable. Her enduring patience and support have been cornerstone of my PhD completion. Special recognition goes to my committee members, especially chair Dr. Jae-Jin Kim, whose leadership and medical and psychiatric expertise has been instrumental. Dr. Dukyong Yoon's insightful inquiries have significantly influenced my project's trajectory, and Dr. Younghee Lee's astute and constructive feedback has broadened my perspective and enhanced my research. Thanks are also due to Dr. JeongGil Ko for his contributions to the computational aspects of my work and for urging me to be bolder and more ambitious as a PhD student.

I would like to acknowledge the children and parents who participated in my studies, without whom this research would not have been possible. I am also indebted to Dr. Soon-Beom Hong and Soyeon Kang, along with the dedicated nurses and administrative staff at Seoul National University Hospital for their assistance with participant enrollment. I extend my appreciation to the Korea Health Industry Development Institute for their financial support of my research. I would also like to express my sincere gratitude to my peers at DHLab, especially the members of Team DiP and Multiomics. I am particularly thankful to Dr. MinDong Sung for providing valuable insights during the initial design of the video data-driven modeling, and to my colleague, Dr. Bo Kyu Choi, who has been with me since the beginning of this journey. Finally, a special note of thanks to my family, whose unwavering trust in me, prayers, and love have been my guiding lights.

연세대학교
YONSEI UNIVERSITY

TABLE OF CONTENTS

연세대학교
YONSEI UNIVERSITY

연세대학교
YONSEI UNIVERSITY

LIST OF FIGURES

연세대학교
YONSEI UNIVERSITY

LIST OF TABLES

연세대학교
YONSEI UNIVERSITY

ABSTRACT

Development and Validation of a Novel Neuro-Behavioral Subclassification System for Autism Spectrum Disorder

Heterogeneity in clinical presentations and underlying neurobiological mechanisms pose significant challenges in delivering personalized interventions for autism spectrum disorder (ASD). With the increasing prevalence of ASD and its growing societal impact, research into subclassifying ASD phenotypes and deciphering unique neurobiological etiologies has gained urgency. In our study, we leverage both retrospective and prospective ASD datasets to construct and validate a multimodal subclassification system. Our multi-modal modeling through integration of features derived from fMRI and behavioral video data aims to identify clusters with distinct clinical and biological profiles.

Utilizing precision-engineered deep learning architectures tailored to each data type – video and fMRI, we successfully extracted key features. Integration of these features followed by the application of advanced clustering techniques for high-dimensional data led to the formation of distinct, data-driven neuro-behavioral clusters. We delineated three clusters: ‘Cluster 3’ with partial impairment in social capacity with the highest overall neural segregation and receiving the strongest genetic influence of the high-deleterious rare coding and non-coding variants; ‘Cluster 2’ with significant autism-related behavioral patterns, abnormal hub node compensation for overall low neural integration and under the effect of less deleterious autism-associated non-coding variants; ‘Cluster 1’ with less evident autism-related behaviors and receiving more genetic contribution of the common variants. The multimodal approach not only enabled the extraction of a broader spectrum of data-driven features to identify clinically distinct subgroups and predict autistic symptom severity, but also enhanced the understanding of individual participants’ neuro-, behavioral-, and genetic profiles, contributing to their unique clinical manifestations. The feature extraction model's explainability was validated by Shapley values.

Our single-source, multi-data approach to creating a multimodal model for ASD subclassification

연세대학교
YONSEI UNIVERSITY

has produced promising results. The reliable clustering obtained from integrated features and thorough validation supports our methodology. Although replication studies are necessary to confirm our findings, this research points to neuro-behavioral clustering as a means to discern biologically distinct groups with unique pathways, significantly impacting personalized treatment strategies aimed at specific genetic, neural, or behavioral challenges.

Key words: autism spectrum disorder, biomarkers, subclassification, multimodal data integration, deep learning

연세대학교
YONSEI UNIVERSITY

1. INTRODUCTION

1.1. Heterogeneity of autism spectrum disorder

Heterogeneity in clinical manifestation and underlying etiologies are major obstacles for identifying key biomarkers in the field of psychiatry and thereby making it difficult for targeted intervention.[1] Psychiatrists and scientists have recognized the limitations of the traditional nosology;[2,3] the past few years, there has been a trend towards partitioning psychiatric heterogeneity into more homogeneous groups—subclassification via various data modalities and data modality specific feature extraction methods.[4,5]

The current research focuses on autism spectrum disorder (ASD), which with its early-childhood onset[6], notable clinical and neuro-biological variability,[4,5,7] and increasing prevalence (0.05% in 1966 to ~2% in 2019)[8,9] calls for the scientific and medical community's attention to the need for and challenges related to subclassification of ASD. The complexity of ASD has also been noted by advances in genomics[7,10,11] and neurobiological studies.[12,13] which have collectively pointed toward multiple etiological pathways. The resulting wide range of clinical and neuro-biological ASD manifestations represents both a challenge and motivation of subclassification, which is necessary for providing personalized interventions for ASD.

1.2. Subclassification methods

Subclassification approaches can be characterized in terms of both the unit(s) of analysis on which variation among individuals is indexed and the nature of the algorithm(s) used to sort individuals into groups.[1] Target units of analyses can be categorized under behavior and biology.[14] The behavior-based units are thought to indirectly index variation of underlying biology and vice versa.[15] Furthermore, quantitative subclassification algorithm can be broadly categorized as supervised (i.e., label driven), unsupervised (i.e., data driven), or their hybrids.[16] These approaches leverage univariate or multivariate statistics, each having advantages and disadvantages.[16]

1.3. Previous ASD subclassification research efforts

연세대학교
YONSEI UNIVERSITY

1.3.1. Behavioral video-based subclassification of ASD

Previously, our group conducted a study that used video-based deep-learning technique to assess joint attention behaviors with the goal of objectively identifying children aged 18-72 months with ASD. The study cohort included 95 children, 45 of whom were clinically diagnosed with ASD.[17] Joint attention describes one's attending to other people and sharing an attentional focus on objects or events with other individuals; early joint attention situations are thought to facilitate learning to socialize.[18,19] We developed a digitalized method for joint attention assessment, which requires a new protocol for specific task administration guidelines to elicit three types of joint attention – initiation of joint attention (IJA), low level response to joint attention (RJA_{low}), and high-level response to joint attention (RJA_{high}) – mentioned in the Early Social Communication Scales (ESCS)[20] for video recording of task-related behaviors. The collected video data were then used as input for training a deep learning (DL) model to identify ASD and assess ASD symptom severity.[17] We found that IJA model performed the best at distinguishing children with ASD from those with ASD. The RJA_{low} and RJA_{high} models also performed well as classifying children with vs. without ASD, but these models did not perform quite as well as the IJA model. Based on these results, we concluded that digital measurement of joint attention may facilitate scalable ASD screening and symptom severity assessment.[17]

Additional analysis on the ASD group from previous study revealed that there may be a correlation between joint attention success rate and either Autism Diagnostic Observation Schedule (ADOS) symptom domain scores for social affect (SA) and restricted repetitive behavior (RRB).[21] Roughly, we could observe four distinct clusters of ASD by their social-communication ability, severity of restricted repetitive behavior, initiation of joint attention, and lastly response to joint attention. In fact, principal component analysis using the four variables revealed that the two types of joint attention contributed to within group variance far greater than either domain score. This is an interesting trend that is worthy of further exploration. Previously various ASD subclassification research utilized difference between the two sub-scores to develop clinically distinct ASD subtypes (i.e. SC>RRB, SC=RRB, RRB>SC) in pursuit of finding new neural and genetic mechanisms that explain such phenotypic heterogeneity.[22,23] Based on sub-analysis using our very own ASD data, perhaps, objective behavior biomarker such as joint attention may be more important in explaining the variance in ASD than human rated clinical scores such as ADOS.

연세대학교
YONSEI UNIVERSITY

1.3.2. Gaze-based subclassification of ASD

Eye-tracker is a popular and frequently used tool for studying ASD characteristics in the context of abnormal sensory systems. To this day, there are several studies that investigated gaze pattern differences between individuals with ASD and those with typical development, which showed intriguing results where individuals with ASD tended to show preference for non-human objects, while those with typical development showed preference for human faces.[24–27] One study explored gaze response to dyadic bids at 2 years, which related to outcomes at 3 years in ASD.[25] In this particular study, the authors were able to perform a cluster analysis in which three clusters or groups of ASD showed varying patterns of eye gaze in terms of which human body parts they tended to view during a social context. One group of ASD that showed least amount of gaze on the face showed the poorest prognosis. Another recent gaze study on ASD revealed that not only are there gaze pattern differences between ASD and TD but also within ASD.[24]

1.3.3. Genomic subclassification of ASD

Although genetic subclassification approaches have provided many new insights about the possible biological mechanisms that are linked with phenotypic heterogeneity, results from these research studies need to be interpreted with much caution. For example, different penetrance between common and rare variants, the low prevalence of any single variant/mutation, although cumulatively all identified ASD-related gene mutations contribute to ~20-40% of clinical non-syndromic ASD, the high genotype-to-phenotype variability, and variable degrees of spatiotemporal convergence across independent risk genes may limit the use of these data to better understand heterogeneity associated with ASD.[28–30] Thus, efforts focusing on discovering clinically relevant subtypes based on genetic approaches alone may not be feasible. Still, recent genetic studies on ASD have shown how a phenotypic spectrum of autism is attributable to the combined effects of de novo mutations, rare variants, polygenic risk and sex.[11] Moreover, there has been a report that different classes of genetic variants have differential impact on phenotypic severity in ASD; while de novo or inherited truncating variants and gene-disruptive copy number variants are associated with more severe forms of ASD, with intellectual disability, variants such as copy number polymorphisms, common

연세대학교
YONSEI UNIVERSITY

variants are associated with ASD individuals with better prognosis and higher intelligence quotient (IQ).[30,31] Such findings may be suggestive of that even though genetic vulnerability does not solely determine and explain for varying clinical manifestations of ASD, its contribution is significant and need to be accounted for. With a growing number of newly discovered gene variants in various ASD whole genome sequence cohorts, there may be a better chance of utilizing such pathway-driven data, perhaps with other complementary data of different modalities to identify new ways to characterize or subclassify ASD.

1.3.4. Neuro-subclassification of ASD

There have been several studies investigating differences in neuroanatomy between individuals with ASD and those without.[1,32] Most of these studies used Autism Brain Imaging Data Exchange (ABIDE) dataset, which is a publicly available dataset of brain imaging data from individuals with ASD and typically developing controls.[33] Hong et al. using this dataset showed that three classes of ASD of three distinct patterns of clinical outcome could be clustered based on cortical thickness, intensity contrast, surface area, and geodesic distance.[32] Choi et al. attempted at subclassification of ASD via an unsupervised clustering method using ABIDE's resting state functional magnetic resonance imaging (rs-fMRI) data.[13] Using 'connectome-based gradient' and 'functional random forest', the authors were able to find subgroups of ASD based on rs-fMRI. Unfortunately, their results were not readily replicable as subgroups resulting from cluster analysis using a replication dataset showed different clinical scores compared to the subgroups that were derived from the discovery dataset. Moreover, the different clusters of ASD individuals did not show significant differences in neural connectivity. Such findings suggest that perhaps purely unsupervised clustering using a complex data such as fMRI may not give way to clinically meaningful subtyping.

1.3.5. Multimodal subclassification of ASD

Recently, many research teams have aimed to use more than one data modality to develop ASD subclassification methods.[23,24,34] EU-AIMS Longitudinal European Autism Project (LEAP) has been accumulating multi-modality data – multimodal MRI, whole genome sequence, eye-tracker, clinical assessment data – from ASD and typical control individuals of European descents and several research teams are tapping on to this multi-modal dataset to better understand ASD more holistically

연세대학교
YONSEI UNIVERSITY

and to develop new methods of subclassification. In one of these studies, Bertelsen et al. took a top-down approach where in which cluster analysis was performed using a scoring system derived from clinical scores, which represent social-communicative—restricted repetitive behavior (SC-RRB) balance as the very first step.[23] By modeling the balance or imbalance thereof between SC and RRB (the two core symptoms of ASD), distinct subgroups of ASD could be identified. Unfortunately, the ASD subgroups resulting from such method did not yield distinct patterns of neural circuitry and genetic components.

1.4. Previous studies' limitations

Cluster analysis via unsupervised learning on complex data such as fMRI did not result in replicable and consistent subclassification; clustering with the replication dataset failed to produce the same ASD subgroups as when clustering with the discovery dataset even while keeping an identical experimental set-up.[35,36] This may be due to relatively small study's sample size, hindering generalizability and replicability; however, another probable explanation would be that without any kind of label to perform the cluster analysis with these individuals were clustered into distinct subclusters solely based on non-linear data patterns—signal patterns devoid of clinical meanings. Concurrently, studies that performed cluster analysis using supervised learning methods failed to produce subgroups of both distinct clinical phenotypes and distinct neuro-biological mechanisms.[23] One should note that these studies employed human rated autism-related scale sub-scores as label for supervised learning. While these human scoring systems are clinically valid and widely used in practice, these human rated scores may not necessarily reflect objective and qualitative differences in phenotype among individuals with ASD. Approaches lacking objective behavioral biomarkers may have limited capacity to segregate heterogeneous ASD populations into distinct subgroups with unique biological underpinnings. A more effective strategy for ASD subclassification involves employing self-supervised learning to derive data-driven features.[37,38] Subsequently, the efficacy and robustness of the feature extraction process can be validated through downstream tasks that utilize clinical scores as labels.

In summary, identifying the most affected ASD neuroscience system level—biology, neural, or behavior—in an individual with ASD to determine the suitable targeted intervention is a significant challenge. Although prior research employing brain imaging, genomics, and clinical assessments

연세대학교
YONSEI UNIVERSITY

has distinguished ASD from typical development, these single modalities fall short in stratifying ASD into distinct neurological, genetic, and behavioral subgroups. Integrating diverse data types, collected from the same individuals, is a rational next step for identifying unique ASD pathways and developing specific treatments. To date, no subclassification models in ASD research have employed such a single-source, multi-modal data approach. An integrated multi-modal subclassification system could enable clinicians to differentiate and treat various ASD types based on a composite profile of system-level abnormalities.

To that end, we conducted a prospective study to develop and validate a neuro-behaviorally driven subclassification system, collecting functional neuroimaging, behavioral video, and genomic data from the same individuals. We aim to synergize resting-state fMRI data, which offers neural-level insights, with joint attention metrics from video data, reflecting behavioral dynamics. The validity of these neuro-behavioral subgroups is verified through clinical presentation, gaze patterns, neural connectivity, and genetic profiles. Additionally, we analyzed the effectiveness of feature extraction from each data modality and assessed whether integrating these modalities enhances our understanding of ASD. Specifically, we evaluated the classification of autism symptom severity based on combined neural and behavioral features using supervised learning, with clinical scores as benchmarks for symptom severity, to determine if the extracted features correspond to clinically significant information.

연세대학교
YONSEI UNIVERSITY

2. MATERIALS AND METHODS

2.1. Retrospective data

2.1.1. Video data

We accessed the 'JointAttention' dataset from our previous study,[17,39] where we had collected video data from 95 individuals for joint attention-based AI model training. Detailed description of 'JointAttention' dataset's participants is presented in the Ko et al. 2022 JAMA Network Open paper. The video data were acquired in a single 10-minute session per participant. Tasks were filmed from a front-facing viewpoint using a Sony DSC-RX100 IV digital camera (resolution: 1920 × 1080, 30 frames/second). Video data for each trial per participant are gathered, pre-processed to remove background, center-cropped, and resized to 224 × 224 pixels. For IJA task, input size of one video is 224x224x300 (30 frames/second x 10 seconds). For RJA task, input size of one video is 224x224x150 (30 frames/second x 5 seconds).

2.1.2. fMRI data

ABIDE is an initiative that compiles rs-fMRI data and related phenotypic information collected across various sites.[40] This data is made available through the Preprocessed Connectomes Project.[41] Data acquisition was performed using a 3.0 Tesla Allegra scanner, adhering to the imaging parameters described in a previous study.[40] The Configurable Pipeline for the Analysis of Connectomes (C-PAC) was utilized to preprocess the data, with the specific steps and settings detailed in the corresponding literature,[42] facilitating appropriate preparation for subsequent analyses. Each brain is partitioned into 39 regions of interest (ROI) based on multi-subject dictionary learning (MSDL) atlas.[43] From the initial dataset comprised of 1,112 scans from 539 individuals with ASD and 573 individuals with TD, removing functional data not meeting the Quality Assessment Protocol standards set by the Preprocessed Connectomes Project community,[41] resulted in a revised dataset of 866 participants, including 402 with ASD and 470 with TD. Further exclusion of individuals lacking valid Autism Diagnostic Observation Schedule (ADOS)[41,44] and full-scale IQ (FSIQ)[41] scores, resulted in a final sample of 750 participants, comprising 282 individuals with ASD and 468 individuals with TD.

연세대학교
YONSEI UNIVERSITY

2.2. Building DL-assisted feature extractors using retrospective data

2.2.1. Video feature extraction DL model

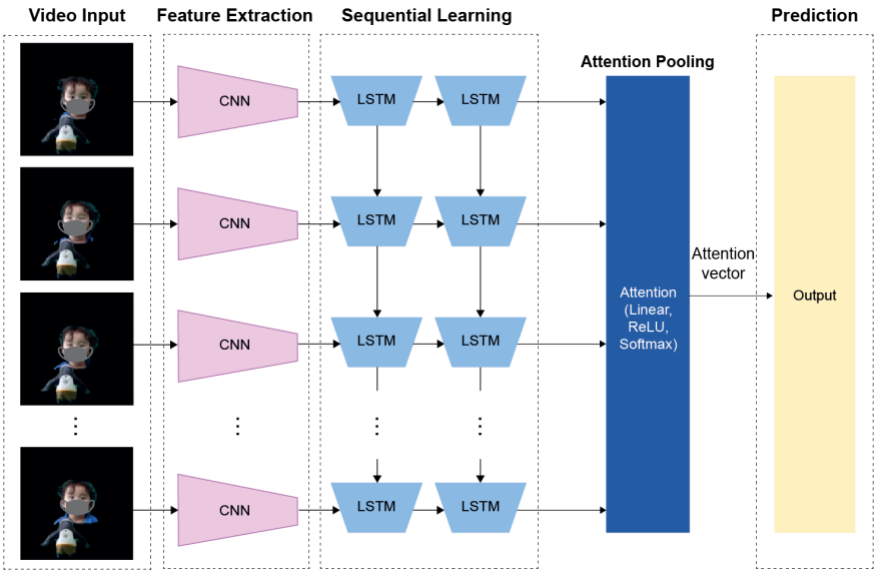

Fig 1. Model architecture for extracting video features

Self-supervised learning method was employed to learn features based on the inherent behavioral features contained in each video rather than clinical variables associated with each participant in the video. Using the methods from Chen et al. SimCLR paper, Normalized Temperature-Scaled Cross-Entropy (InfoNCE/NT-Xent) loss was used which allows for contrastive learning of visual representations.[44] Two separate data augmentation operators are sampled from the same family of augmentations ($t \sim T$ and $t' \sim T$) and applied to each data example to obtain two correlated views. A base encoder network – in our case Convolutional Neural Network (CNN)-Long Short-Term Memory (LSTM)-Attention (Fig. 1) – f(•) and a projection head g(•) are trained to maximize agreement using a contrastive loss. After training is completed, we throw away the projection head g(•) and use encoder f(•) and representation h for downstream tasks—training with our newly acquired prospective dataset. The video dataset was split 8:2 for training and validation of deep learning model over 100 epochs.

연세대학교
YONSEI UNIVERSITY

2.2.2. fMRI feature extraction DL model

2.2.2.1. Graph node feature engineering

Functional connectivity matrices are widely utilized in rs-fMRI research to extract statistical correlations from fMRI blood-oxygen-level-dependent (BOLD) signal time-series data, providing framework for understanding brain interactions in downstream tasks.[45,46] However, their dimensionality reduction can oversimplify data, potentially losing insights about individual brain region's activity and nonlinear connectivity between brain regions[47] and masking the functional network's intricate variability across time.[48] An alternative, employing advanced feature engineering to extract multifaceted features from BOLD time-series[49] – such as time-frequency features via continuous wavelet transform (CWT)[50–52] – can inform graph-based analyses for a more detailed representation of connectivity. CWT is an established method in bio-signal analysis[50,51,53] that decomposes signals into localized wavelets for time-frequency analysis.[53] Unlike the Fourier transform, the CWT excels in analyzing non-stationary frequencies over time.[52] The CWT generates a two-dimensional time-frequency representation by convolving the signal with scaled and translated version of a mother wavelet, providing local frequency information over time. Each participant's CWT data, initially derived from time-series signal data across 39 ROIs, are transformed into scalogram images,[50] which are then fed into a CNN (Resnet18) framework to extract the corresponding CWT features.[51]

2.2.2.2. CWT-based graph neural network architecture for feature extraction

Graph Neural Networks (GNNs), well-suited for spatially structured, relational data, [48] can be enhanced by feature engineering preprocessing that enable the capture of complexities related to time, frequency, and spatial-structure.[54–56] Our custom GNN architecture includes a feature-engineering step that extracts CWT from the BOLD signal time-series for each ROI and training step, where these preprocessed features are then integrated into the GNN using the spatial coordinates of each ROI as baseline edge information. Thereafter, with each iteration the weights of the 741 edges (total number of edges of complete graph consisting of 39 nodes) are updated based on different features. The 39 nodes' updated weights based on training are concatenated to perform graph-level binary classification. The same SimCLR loss function was used to conduct contrastive learning similar to the method employed for training and extracting features from video data. The GNN with pre- feature engineering step is presented in Fig 2.

연세대학교
YONSEI UNIVERSITY

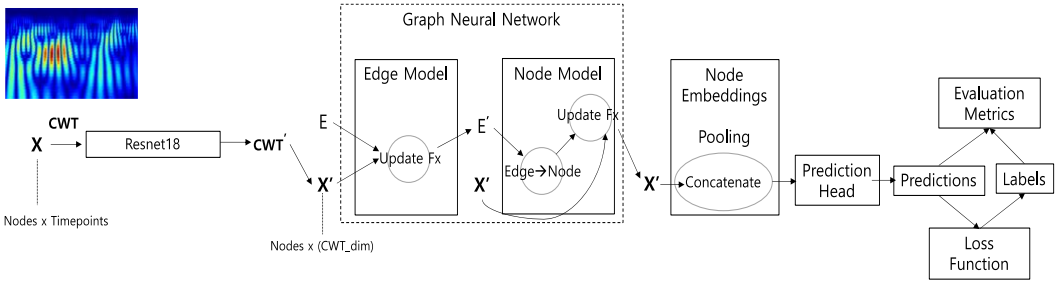

Fig 2. Model architecture for extracting fMRI features

2.3. Prospective data

2.3.1. Participant enrollment

Enrollment for a prospective cohort study was conducted from the Child and Adolescent Psychiatry Division of Seoul National University Hospital. The research protocol was approved by the Seoul National University Hospital IRB Review Board (IRB No. H-2210-137-1374). Enrollment criteria are: 1) age of 48~71 months, 2) male, 3) children diagnosed with ASD by a psychiatrist and confirmed by ADOS2. Exclusion criteria are: 1) receiving pharmacological treatment, 2) having comorbid neuropsychiatric conditions such as developmental coordination disorder, attention deficit hyperactivity disorder, etc.

2.3.2. Clinical assessments

The diagnosis of ASD is confirmed using Autism Diagnostic Observation Schedule II (ADOS-2),[21] the gold standard diagnostic tool for ASD diagnosis. Autistic tendencies are measured using the Korean versions of the Social Responsiveness Scale (K-SRS) as well as Social Communication Questionnaire (K-SCQ).[57] The SRS is a 65-item questionnaire that asks parents and/or teachers about the characteristics of the social interactions shown by children over the past 6 months.[57] Each question is scored from zero to three points, depending on the frequency of the action described in each item. Higher scores mean a lower social function. The SCQ is a 40-item screening instrument that is based on Autism Diagnostic Interview-Revised (ADI-R), a tool for more in-depth assessment of ASD symptoms, and selects key items that deviate from normal development.[57] Child behavioral

연세대학교
YONSEI UNIVERSITY

problems were checked with Child Behavior Checklist (CBCL) as well as Vineland Adaptive Behavior Scale (VABS).[58] The child's motor functions were assessed through Developmental Coordination Disorder Questionnaire (DCDQ).[58] To assess the cognitive levels of participants, the Korean Wechsler Preschool and Primary Scale of Intelligence–Fourth Edition (K-WPPSI-IV) was be used.[59]

2.3.3. Joint attention tasks and video data acquisition

2.3.3.1. Initiation of joint attention

The initiation of joint attention (IJA) task was designed as follows. A rotation of age- and culture-appropriate tests toys, which were selected following the guidelines of the ADOS-2[60] and Mundy's ESCS manual (10 different types or shapes of similar size: width × length × height = 3 cm × 5 cm × 3 cm), was placed along the midline, 70 cm away from the edge of the table at which the child was seated. If the toy was placed too close to the child, they would simply pick it up and play with it without making any effort to interact with the examiner. A trained examiner was seated adjacent to where the toy was placed, such that the child could see the examiner's face by making an approximately 45-degree head turn or by shifting their gaze considerably to their right. The experimental process was as follows: the examiner placed a toy at the designated spot, waited for 30 seconds, and simply faced the child without providing verbal instructions. Once the child initiated joint attention by shifting their gaze from the toy to the examiner and back to the toy (sometimes also pointing at the toy), the examiner was asked to shift their gaze or turn their head to the toy to match the child's response. This task was repeated once more with the same toy after a 30 second pause, and then a different toy was introduced. The order of the toy presentation was pseudo-randomized across participants. If the children failed to show any interest in the toy after 30 seconds, the examiner could use an alternate toy.

2.3.3.2. Response to joint attention

Response to joint attention (RJA) tasks were designed to observe whether a child would direct and maintain their attention on an object to which the examiner pointed with their index finger. Depending on the distance between the examiner's index finger and the object, the RJA tasks were further divided into RJA_{low} (near) and RJA_{high}(far) tasks, where RJA_{low} involved the examiner pointing to toy objects on the table and RJA_{high} involved the examiner pointing to poster pictures on

연세대학교
YONSEI UNIVERSITY

the walls. The RJA_{low} task utilized stimuli similar to that of the initiation of joint attention task, except that two toy objects (one as a stimulus and the other as a distractor) were used. Four posters depicting a child-friendly image (a car, butterfly, bananas, and puppy) covering half of an A4 sheet were pasted onto three walls—left, right, and behind—with respect to where the child participant was seated. Each poster was approximately 100 cm from the child's position. The three types of joint attention are illustrated in Fig 3.

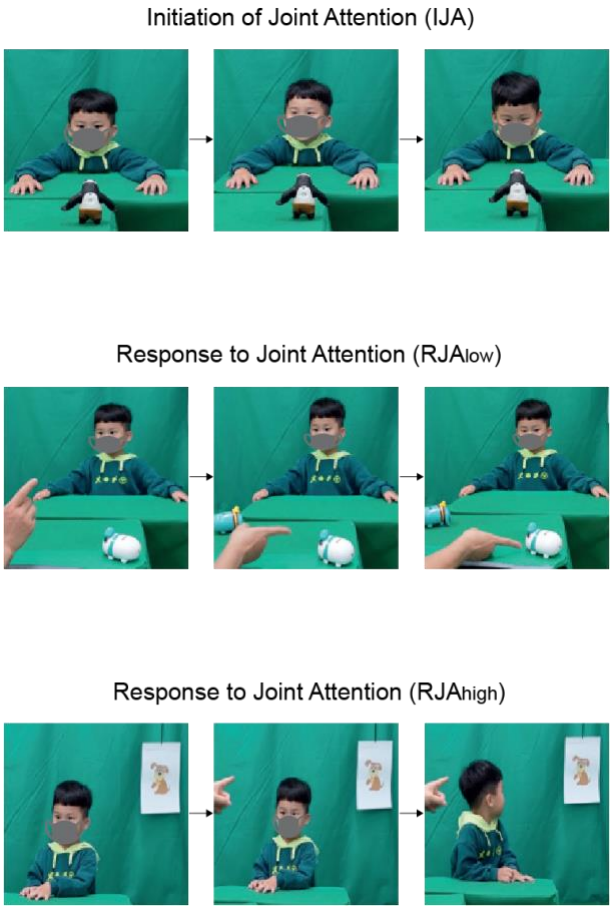

Fig 3. The different types of joint attention tasks

연세대학교
YONSEI UNIVERSITY

2.3.4. Setup for joint attention experiments based on our protocol

Initiation of joint attention (IJA) tasks required use of only toy 1, while response to joint attention tasks, low (RJA_{low}), required the use of toy 1 and toy 2 (distraction), and response to joint attention tasks, high (RJA_{high}), required use of pictures 1–4 as shown in Fig 4.

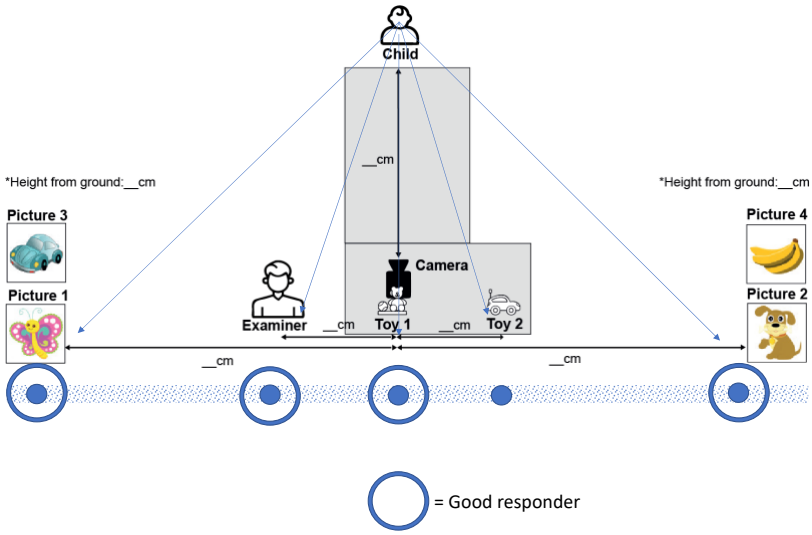

Fig 4. Joint attention task-video data acquisition set-up

2.3.5. Video data pre-processing for model training and feature extraction

Same method was used to pre-process the video data as that used in Ko et al. 2022 paper.[39]

2.3.6. fMRI data acquisition

Brain imaging data was collected on 3T Siemens Tim Trio Systems scanner at Seoul National University Hospital. Resting state fMRI scans were acquired using a standard gradient-echo echo planar imaging paradigm: FOV of 220 x 220mm (64 x 64 matrix), TR=2s, TE=30ms, FA= 77°, 162 vol, 32 sequential ascending axial slices of 4mm thickness and 1mm skip. Participants were sedated and had their eyes closed during the scan. Data were processed using C-PAC preprocessing

연세대학교
YONSEI UNIVERSITY

pipeline,[42] which include slice timing correction, motion correction, intensity normalization, nuisance signal removals, such as respiration, heartbeat, low-frequency scanner drifts, global mean signal regression, head motion, etc. The preprocessed data were band-pass filtered (0.01-0.1 Hz) and spatially registered to MN152 template space. ROI time series data will then be extracted from the resulting fMRI images using the MSDL brain atlas.[43]

2.3.7. Genomic data acquisition

2.3.7.1. Whole genome sequencing

Whole genome sequencing (WGS) was performed on peripheral blood samples from 31 participants with autism spectrum disorder (ASD) using the NextSeq 550Dx System (Illumina, San Diego, CA, USA). Excluding participant ASD010, 29 samples were analyzed. The WGS was conducted by TheragenBio with a custom quality control sequence analysis pipeline. Variants were identified using HaplotypeCaller and MuTect2 from the GATK package (3.8-0) and VarScan2 (2.4.0).

2.3.7.2. Filtering and annotation

The VCF (Variant Call Format) files representing 29 participants were initially filtered using GATK Variant Filtration, applying a filter to PASS, with a Mapping Quality (MQ) greater than 30 and Read Depth (DP) exceeding 10 to ensure high-quality variant selection. Further filtering and annotation processes were conducted using Python and Java scripts to distinguish between common and rare variants, defined by allele frequency (AF). Common variants, identified as those with AF greater than 1%, were used for subsequent polygenic risk score (PRS) calculations. The VCF files were normalized, and PLINK binary files were prepared using Bcftools.

2.3.7.3. Polygenic risk score calculation

To calculate the PRS for various conditions, including ASD, ADHD, schizophrenia (SCZ), educational attainment (EA), and intelligence, the filtered variants were processed using PLINK 1.9 and Bcftools. Initially, indels and multiallelic variants were excluded, and the variants were normalized to generate PLINK binary files. The input files were then merged. Reference data for PRS calculation included refined Genome-Wide Association Study (GWAS) data for the aforementioned conditions. Clumping was performed to sort single nucleotide polymorphisms

연세대학교
YONSEI UNIVERSITY

(SNPs) based on linkage disequilibrium and p-values, followed by the extraction of index SNP IDs. A range-list file containing different p-value thresholds for SNP inclusion in the PRS was created. PRS scores were then calculated using the prepared binary files, refined GWAS data, range-list files, SNP p-values, and extracted SNP IDs, resulting in comprehensive PRS profiles for each participant across multiple conditions.

2.3.7.4. Annotation of rare variants

For rare variants (AF less than 1%), annotation included both coding and non-coding regions. Coding region variants were annotated using tools and databases such as pLI (probability of being Loss-of-function Intolerant), CADD (Combined Annotation Dependent Depletion), SIFT (Sorting Intolerant From Tolerant), PolyPhen (Polymorphism Phenotyping), and the SFARI gene list. Non-coding region variants were annotated using databases including the Enhancer Atlas, HACER, and the Promoter Atlas provided by the FANTOM5 project, with CADD scores used to assess their significance. This comprehensive annotation ensured a detailed understanding of both common and rare variants, contributing to the robust analysis of genetic factors in ASD.

2.3.8. Feature extraction using pretrained model weights

Using the pretrained deep learning model architectures and pretrained weights using retrospective dataset, we fine-tuned or further trained using preprocessed prospective data per data modality (video and rs-fMRI). The same loss function (InfoNCE/NT-Xent) was utilized as the pretraining phase, for at least 50 epochs and upon completion of training, feature vectors were stored for downstream tasks.

2.4. Prospective data cluster extraction via retrospective clustering algorithm

Prior to performing multi-modal clustering analysis using prospective cohort dataset, we conducted clustering analysis using the retrospective cohort datasets to build a clustering algorithm for the “behavioral clusters” and “brain clusters”. For the video data, indirect measures of gaze patterns using computer vision-derived variables computed from face landmark variability such as ‘yaw’, ‘pitch’, ‘roll’, ‘kurtosis’, and ‘skewness’ were utilized. Face landmark localization on collected videos was feasible using face detection algorithms provided by Dlib library.[61] Rotation matrix to

연세대학교
YONSEI UNIVERSITY

Euler angles conversion algorithms were used to impute 'yaw', 'pitch', and 'roll.' Due to the curse of dimensionality principal component analysis and k-means clustering method was employed to develop a clustering algorithm based on these behavioral patterns observed in large retrospective dataset. This process was repeated using the ABIDE dataset: using the edge connectivity features derived from the trained GNN model results for each participant, clustering algorithm was developed after principal component analysis and k-means clustering was applied. Then, on the prospective dataset, these "gaze-based clusters" and "brain connectivity clusters" algorithms were applied onto the prospective video and rs-fMRI datasets to assign clusters based on patterns learned from retrospective datasets. This clustering information was then integrated into the multi-modal model.

2.5. Multi-modal data integration for downstream tasks

Various multimodal integration techniques have been introduced to utilize data from different modalities such as fMRI, SNP, clinical data for the purpose of developing a machine-learning model for disease detection.[62] Depending on the stage at which the data integration occurs, there may be early, intermediate, and late phase multimodal integration approaches. Late phase approach is where separate machine-learning model is trained for each type of data then predictions of different models are combined to make a final decision.

Early data fusion works best for integrating data types sharing the same number of dimensions such as different MRI modalities. In this study, we utilized late-stage integration treating the different data types separately, processing each using appropriate preprocessing and feature extraction pipeline, then latent vectors derived from each modality are concatenated then an ensemble (voting) classifier predicts outcome.[63] One machine learning classifier (XGBoost)[64] and a fully connected multi-layer perceptron (MLP)[64] were utilized to learn from the integrated features from video and rs-fMRI data sources for the purpose of clustering and autism symptom severity classification. Similarity network fusion (SNF)[65] was employed for data integration—method that allows for integration of different data modalities by using networks of samples. Initially, similarity matrices are created for each data type for each participant, then these matrices are fused through iterative processes over a wide range of SNF hyperparameters (k-nearest neighbors weighted similarity kernel; K and u) until convergence (z-Rand similarity index), ensuring stable integration.[65] The

연세대학교
YONSEI UNIVERSITY

final output is a co-assignment matrix, which represents the combined similarity across all nodal measures; this integrated network is subsequently used for spectral clustering based on optimal parameters.[65] The overall process of data integration and downstream tasks are visually represented in Fig 5.

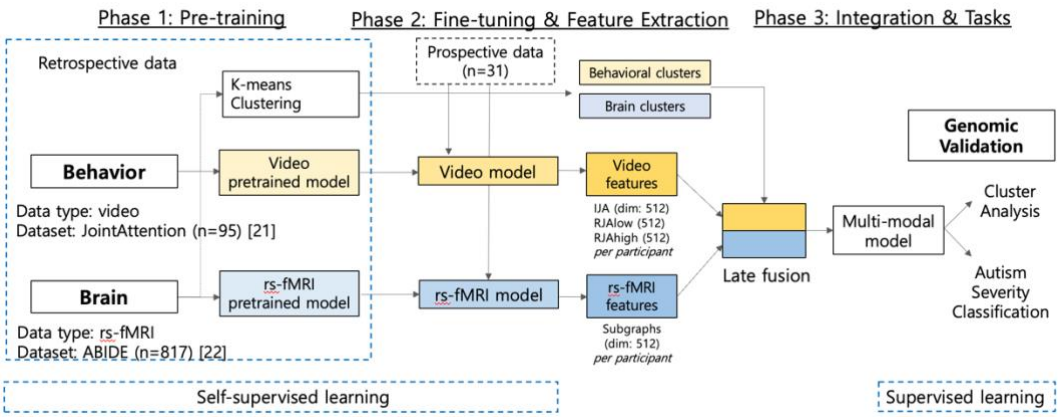

Fig 5. Overall study design and modeling of multi-modal system

2.6. Cluster analysis

2.6.1. Clustering methods

Two clustering methods were utilized: K-means clustering and SNF-based spectral clustering followed by hierarchical clustering. K-means was applied to dimension-reduced feature vectors of the 3456 combined features (consisting of both video and fMRI) via PCA. The SNF-based clustering used the final co-assignment matrix, leveraging cosine similarity across all nodal measures. Spectral clustering was employed to identify a pre-specified number of subgroups (i.e., 3). Hierarchical clustering was then performed on the final co-assignment matrix to identify subgroups across a range of clusters (2-10). A dendrogram was constructed, and the optimal number of clusters was determined using the Calinski-Harabasz index.[66] This comparative approach aims to determine the more effective clustering method for the same set of individuals.

연세대학교
YONSEI UNIVERSITY

2.6.2. Genetic validation of multi-modal clustering

After neuro-behavioral clustering was conducted, SNP information gathered from each sample were used to compare the genetic profiles among the different neuro-behavioral clusters. Furthermore, the Human Protein Atlas (https://www.proteinatlas.org/) was utilized to understand how having certain genetic variant contributed to abnormal neural connectivity evidenced by the rs-fMRI GNN model outcomes.

2.7. Autism symptom severity prediction

Lastly, we addressed the task of classifying autism symptom severity using the ADOS-2 calibrated total scores, ranging from 0-4 for non-to-mild severity and ≥5 for moderate-to-severe autism. This classification was performed using both an XGBoost classifier and a custom MLP model. The objective was to evaluate whether integrating multi-modal information from distinct data modalities—behavioral and neurobiological—enhances the model's predictive performance in identifying levels of autism symptom severity. This investigation also aimed to substantiate the utility of multi-modal clustering or subclassification. The premise is that richer, more diverse information sources facilitate the grouping into more finely delineated, targeted subcategories. Additionally, we explored the potential for predicting clinical scores—which assess the severity of autism—through a composite of objective behavioral assessments and neurobiological data. This approach could also reveal the relative contributions of behavioral and neurological factors to the overall clinical symptom severity. Such insights are invaluable for designing tailored intervention plans that are specific to the patient's characteristics, potentially enhancing therapeutic outcomes.

2.8. Statistical analysis

2.8.1. Power calculation – sample size estimation

For this exploratory study, the lack of preceding data precludes the establishment of a definitive sample size. Nevertheless, referencing guidelines for comparable studies, we advocate a minimum sample size of 12[67], considering the study's feasibility, precision of means and variances, and compliance with regulatory requirements. Reflecting on a previous investigation that effectively classified three distinct severity subclasses of ASD with a cohort of 45 individuals[17], our study plans to recruit 60 participants. This number takes into consideration potential participant dropouts or

연세대학교
YONSEI UNIVERSITY

missing data essential for statistical analysis.

2.8.2. Evaluation of effective clustering using metric scores

To validate or determine the effectiveness of clustering mythology employed, metrics such as Silhouette Score,[68] Davies-Bouldin Index,[69] and Cluster Stability[70] were used. Silhouette score measures how similar an object is to its own cluster compared to other clusters; Davies-Bouldin index evaluates the clustering algorithm by taking the average similarity measure of each cluster with its most similar cluster, where similarity is the ratio of within-cluster distances to between-cluster distances. Cluster stability allows for evaluating stability of clusters over multiple runs with different subsets of the data to check the robustness of clustering.

2.8.3. Evaluation of multi-modal autism symptom severity prediction

Multi-modal model's classification performance was evaluated using area under the receiver operating characteristics (AUROC), accuracy, precision, and recall.

2.8.4. Cluster characteristics

Group comparison among the different clusters were statistically analyzed. Clinical characteristics, eye-gaze patterns (head movement response to joint attention induction – 'yaw', 'pitch', 'roll', 'kurtosis', and 'skewness'), rs-fMRI profiles (top 5 nodes of importance and 1 or 2-step eigenvector centrality), number of ASD-associated (with high CADD score) coding and non-coding genes, the ratio between coding to non-coding gene variants, the ratio between common and rare variants, and polygenic risk scores for ASD. Means, standard deviations, medians, and ranges is used to express continuous variables. The chi-squared test is used to compare categorical variables. Statistical analyses and calculations of the validation measures are performed using Python 3.9.12 with SciPy version 1.13.1 and Statsmodels 0.14.1. The threshold for statistical significance was set at $p<0.05$.

연세대학교
YONSEI UNIVERSITY

3. RESULTS

3.1. Participant characteristics

3.1.1. Retrospective datasets

Using dataset from our previous project 'JointAttention,' which was geared towards building a video-based deep learning model for predicting ASD vs typical development (TD) as well as symptom severity by ADOS total calibrated scores (CSS) include total of 95 individuals – where 58 showed non-mild ASD symptom severity (ADOS total css≤4) and 37 showed moderate to severer (ADOS total css>4). ABIDE dataset was used for developing deep learning model for extracting rs-fMRI features. From the preprocessed ABIDE database, only participants with available ADOS scores were included for analysis and model training, which were 817 in total, 470 meeting criteria for non-mild and 347 individuals meeting criteria for moderate to severe ASD.

3.1.2. Prospective dataset

SNU dataset included total of 31 participants, 9 of whom met criteria for non-mild ASD and 22 meeting criteria for moderate to severe ASD.

3.1.3. Clinical characteristics of participants across retrospective and prospective datasets

The clinical characteristics of participants across retrospective and prospective datasets are shown in Table 1. While the JointAttention and SNU datasets showed a similar severity range, of overall mean (SD) ADOS total css scores of 6.1 (1.6) and 6.4 (2.4), respectively; ABIDE dataset's overall average ADOS total css score was that of 2.79 (2.48). Such class (severity) imbalance could contribute to imbalanced class representation, rendering difficult to perform transfer learning using symptom severity score as label. Furthermore, FSIQ was overall higher for ABIDE dataset compared to the other datasets.

연세대학교
YONSEI UNIVERSITY

Table 1. Participant characteristics across datasets

	Retrospective datasets						Prospective dataset		
Database	**JointAttention [21]**			**ABIDE [22]**			**SNU**		
Group by Severity	Non-Mild (N=58)	Moderate-Severe (N=37)	Overall (N=95)	Non-Mild (N=523)	Moderate-Severe (N=227)	Overall (N=750)	Non-Mild (N=9)	Moderate-Severe (N=22)	Overall (N=31)
Age Mean (SD)	4.04 (1.02)	3.93 (1.17)	(4.0, 1.08)	16.8 (7.20)	16.8 (7.69)	16.8 (7.35)	4.2 (0.7)	4.3 (0.8)	4.2 (0.7)
Sex, n(%) Male	31 (53.4)	20 (54.1)	51 (53.7)	426 (81.5)	204 (89.9)	630 (84.0)	9 (100.0)	18 (100.0)	31 (100.0)
FSIQ Mean (SD)	98.3 (23.3)	57.5 (19.0)	82.4 (29.4)	111 (12.2)	105 (16.3)	109 (13.9)	84.3 (24.2)	63.4 (26.0)	69.7 (26.9)
ADOS CSS* Mean (SD)	3.8 (0.5)	6.6 (1.3)	6.1 (1.6)	1.23 (0.70)	6.40 (0.699)	2.79 (2.48)	3.1 (0.3)	8.0 (1.2)	6.2 (2.4)

* Non-Mild (ADOS Total CSS≤4), Moderate-Severe (ADOS Total CSS >4)

3.2. Multi-modal clustering results

As a result of clustering using integrated features from MLP model, using K-means clustering, optimal k = 3 based on elbow method. Across 5 folds, fold 3 showed the highest silhouette score of 0.132 (0.0612-0.132), which is considered poor clustering. Based on Calinski-Harabasz index, the optimal number of clusters based on SNF followed by hierarchical clustering was also 3. The SNF plus hierarchical clustering fared much better. For k=12, 5 iterations, the best fold (fold 3)'s silhouette score was 0.639 (0.396-0.639) and the adjusted Rand Index was 1, which is considered very good. Hence, the cluster analysis to explore the differences in clinical characteristics, neural connectivity and genetic profile were done using the clusters discovered using SNF plus hierarchical clustering. The list of participants belonging to each cluster are shown in Table 2. The similarity network fusion for aggregating feature vectors of video and rs-fMRI is presented graphically in Fig. 6 and the visualization of the result of hierarchical clustering is shown in Fig. 7.

연세대학교
YONSEI UNIVERSITY

Table 2. SNF plus hierarchical clustering-based neuro-behavioral clusters

Clusters (total N=31)	**Participant ID**
Cluster 1 (N=6)	asd001, asd002, asd013, asd014, asd036, asd038
Cluster 2 (N=5)	asd017, asd024, asd025, asd027, asd031
Cluster 3(N=20)	asd003, asd005, asd006, asd007, asd008, asd009, asd011, asd012, asd015, asd016, asd018, asd019, asd021, asd022, asd023, asd026, asd028, asd029, asd030, asd035

3.2.1. Clinical manifestations of neuro-behavioral clusters

The clinical differences of the three neuro-behavioral clusters are shown in Table 3. The characteristics of each cluster are indicated by arrows, which depict the severity and quantity of specific symptoms, with upward arrows indicating an increase in severity. These results reflect the clinical characteristics of each cluster and facilitate a clearer understanding of the various aspects of ASD. The data is presented as median values with the first and third quartiles. While there were no significant differences in the ADOS scores (severity scores) among the three groups, differences in other clinical manifestations were noted.

Cluster 1 displayed mild autism symptoms with lower scores in social interaction. This group showed high intelligence and no significant impairments in language delay or visual information processing abilities, maintaining capabilities necessary for daily living. Video data revealed well-preserved social skills in initiating social interactions during joint attention tasks, and their responsiveness to social cues was nearly at the level of typically developing children.

연세대학교
YONSEI UNIVERSITY

Cluster 2 was the most deficient group in terms of social interaction, especially in social communication skills, and showed the most pronounced intellectual disabilities. This cluster had significant deficits in language development and visual information processing abilities, and motor skill development was impaired, reducing their ability to coordinate movements. Their overall performance in video tasks was poor, marking this group as having the most distinct overall social deficits and developmental delays related to autism.

Cluster 3 consisted of children with social communication abilities that were inferior to those in Cluster 1 but milder compared to Cluster 2. However, this group displayed various functional impairments in daily living activities, especially in fine motor skills. In video tasks, their ability to respond to social signals was somewhat better preserved compared to their ability to initiate social interactions voluntarily. This group might require further investigation into underlying pathways that could be causing adaptive behavior issues and other autism-related symptoms.

Table 3. Clinical manifestations of neuro-behavioral clusters

Clinical scores	**Cluster 1 (N=6)**	**Cluster 2 (N=5)**	**Cluster 3 (N=20)**	**p-value**
ADOS total* ↑ Median [Q1, Q3]	7.0 [4.0,7.8]	7.0 [6.0,8.0]	7.0 [3.8,9.0]	0.889
SRS comm** ↑ Median [Q1, Q3]	12.0 [12.0,37.0]	35.0 [29.0,47.0]	27.5 [20.0,37.0]	0.272
SRS motivation** ↑ Median [Q1, Q3]	7.0 [6.0,17.0]	15.0 [12.0,20.0]	14.0 [8.8,22.2]	0.523
FSIQ§ ↓ Median [Q1, Q3]	76.0 [74.0,86.0]	56.0 [42.0,63.0]	65.0 [43.2,99.0]	0.379

연세대학교
YONSEI UNIVERSITY

VCI§ ↓ Median [Q1, Q3]	83.0 [59.0,83.0]]	53.0 [53.0,62.0]	62.0 [45.0,107.0	0.571
VSI§ ↓ Median [Q1, Q3]	87.0 [85.0,96.0]	67.0 [64.0,70.0]	79.0 [67.0,94.5]	0.205
VABS daily‡ ↓ Median [Q1, Q3]	80.0 [80.0,85.0]	80.0 [63.0,80.0]	74.0 [69.5,88.5]	0.275
VABS social‡ ↓ Median [Q1, Q3]	83.0 [73.0,92.0]	58.0 [48.0,60.0]	56.0 [51.5,83.0]	0.045
DCDQ fine motor‡ ↓ Median [Q1, Q3]	10.0 [8.0,10.0]	12.0 [5.0,14.0]	7.0 [5.0,13.5]	0.857
DCDQ coord‡ ↓ Median [Q1, Q3]	16.0 [15.0,16.0]	6.0 [5.0,8.0]	10.5 [8.8,14.0]	0.11
IJA success(%)† ↓ Median [Q1, Q3]	77.5 [52.5,95.0]	35.0 [30.0,35.0]	40.0 [13.8,55.0]	0.072
RJA_{low} success(%)† ↓ Median [Q1, Q3]	50.0 [37.5,62.5]	25.0 [20.0,35.0]	57.5 [20.0,76.2]	0.372
RJA_{high} success(%)† ↓ Median [Q1, Q3]	93.8 [91.7,99.0]	66.7 [62.5,95.8]	81.2 [64.4,96.2]	0.226

↑,↓ Symptom is more severe in the direction of arrow

* Currently available tool used for classifying ASD, † Our proposed method of behavioral classification

** Autism-associated traits

§ FSIQ: full scale intelligence; VCI: verbal comprehension, VSI: visuospatial index

‡ VABS: Vineland Adaptive Behavior Scales (adaptive function); DCDQ: developmental coordination disorder quesetionnaire (motor function)

3.2.2. Joint attention performance in neuro-behavioral clusters

연세대학교
YONSEI UNIVERSITY

Higher initiation of joint attention success rates was observed in cluster 1, which is suggestive of that individuals belonging to cluster 1 tend to show less impaired initiation of joint attention, which could translate to greater motivation or need for social interaction. There was statistically significant difference in IJA performance between cluster 1 and cluster 3; thought not statistically significant, cluster 1 performed better at IJA compared to cluster 2 as well. Overall, response to joint attention were low across all clusters and no statistically significant difference was observed. However, cluster 3 showed trends of improvement from IJA during RJA_{low} task. These results are shown graphically in Fig 6.

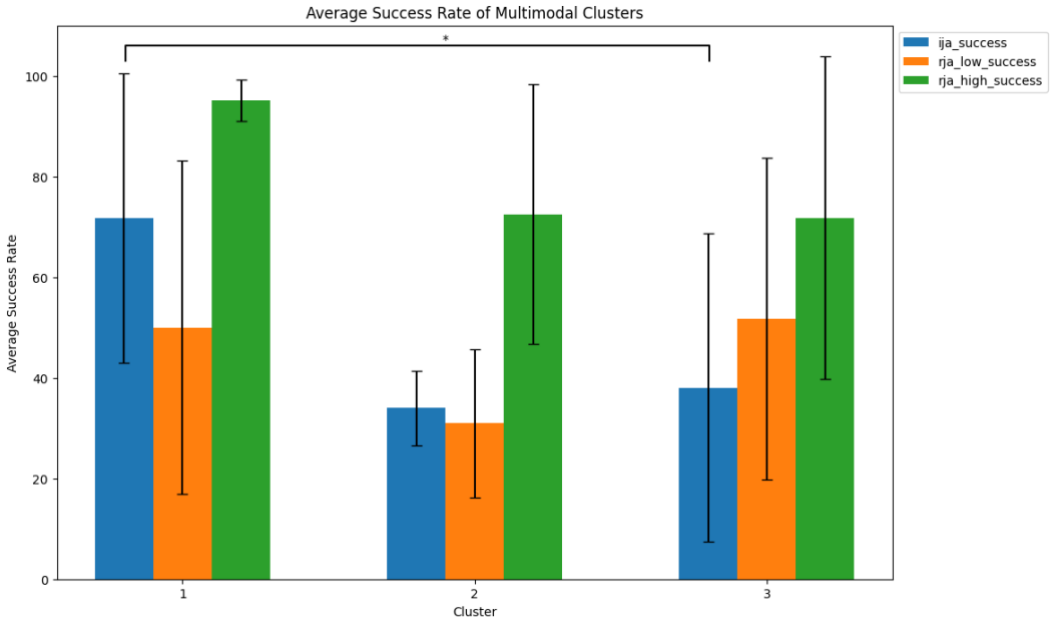

Fig 6. Joint attention performance in neuro-behavioral clusters

3.2.3. Gaze pattern analysis in neuro-behavioral clusters

In the context of head pose estimation, variables such as pitch, yaw, roll, skewness, and kurtosis were utilized in cluster analysis, illustrated via parallel coordinates to distinguish patterns by cluster. The mean roll (head tilt left/right) differed significantly across the three clusters. Cluster 1 showed

연세대학교
YONSEI UNIVERSITY

consistent left tilt, indicating a preference to face the examiner during the initiation of joint attention tasks. In contrast, cluster 2's right tilt might be interpreted as facing away from examiner, highlighting decreased need for initiating social interaction. Cluster 3 showed a balanced head tilt, which may mean indecisiveness or flexibility in engagement. Cluster 2 showed significantly lower skewness suggests a more consistent or repetitive head tilting pattern, indicating less variability in their head movements. Cluster 1 and 3 showed higher skewness suggesting more varied head movements. Cluster 2 with lower variability in head movements could be indicative of more rigid or restricted social interaction patterns. Cluster 1 showing higher kurtosis could indicate more pronounced peaks in yaw movements, suggesting occasional but significant head turns. Cluster 2 and 3 with lower kurtosis could mean more evenly distributed yaw movements, suggesting less pronounced head turns and less reactivity during RJA tasks. Cluster 2 showed negative yaw skewness, which is suggestive of a tendency towards more consistent head movement in one direction. Cluster 1 and 3 that show positive skewness may mean a broader range of head movements. These gaze (head pose) patterns in neuro-behavioral clusters are represented in the following figures– Fig 7.

연세대학교
YONSEI UNIVERSITY

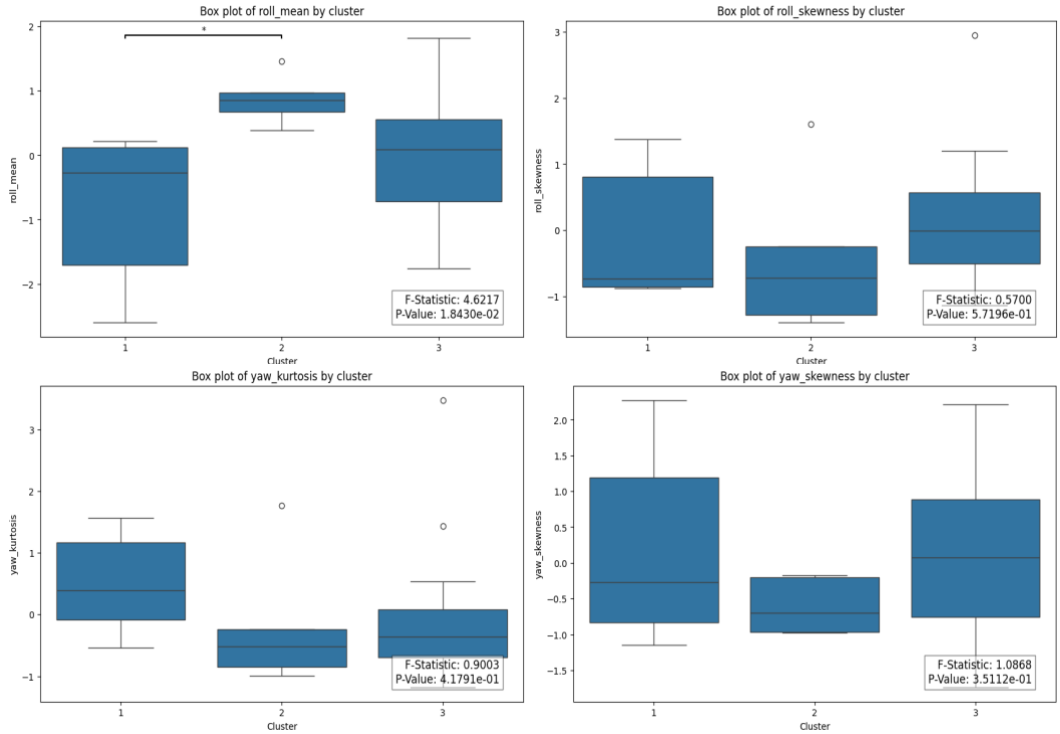

Fig 7. Mean roll, roll skewness, yaw kurtosis, and yaw skewness in neuro-behavioral clusters

3.2.4. Neural connectivity analysis in neuro-behavioral clusters

3.2.4.1. PageRank-based node importance by clusters

Self-supervised learning of GNN using feature engineering steps initially on the ABIDE dataset and then transfer learning on our prospective dataset for over 5 folds yielded updated edge weights for 741 edges connecting the 39 fully connected nodes. Applying PageRank, informed by edge weights from model training, revealed key nodes that the Graph Neural Network (GNN) model identified as critical features. For the 5 folds for fold 0, 2, 3 all showed right temporoparietal junction (R TPJ) to be the most important node for clustering the rs-fMRI data as shown in Table 4. The other two nodes were left insula and left anterior intraparietal sulcus.

3.2.4.1.2. Segregation and integration as measures of neural connectivity

In the graph-theoretic and GNN architecture evaluation of brain networks, which encompass 39

연세대학교
YONSEI UNIVERSITY

regions of interest from a multi-subject dictionary learning atlas, nodes were engineered using retrospective data and then applied prospectively in a self-supervised manner. The overall clustering coefficient and eigenvector centrality were calculated, particularly focusing on key nodes like right TPJ, left insula, and left anterior intraparietal sulcus, identified via 5-fold cross-validation as critical in distinguishing the clusters. The neural connectivity analysis results using hub nodes are shown in Table 5. Clusters 2 and 3 showed higher segregation compared to Cluster 1, indicating more specialized and tightly knit networks. Cluster 2 displayed high segregation but also showed signs of increased integration, possibly due to compensatory mechanisms at R TPJ, which could be contributing to behavioral and developmental delays. Cluster 3, showing the highest segregation and a lack of compensatory integration, indicated reduced cooperative interactions among brain regions, potentially leading to impairments in adaptive behaviors necessary for daily living.

Table 4. Hub nodes of ASD participants from retro-, prospective datasets

Fold number for GNN–SSL (retro- & pro-spective dataset)	**Top node with most influence in neural connectivity**
Fold 0	Vis, R TPJ*
Fold 1	L Ins
Fold 2	R TPJ
Fold 3	R TPJ
Fold 4	L Ant IPS

*Top two nodes with highest model weights, thereby contributing most to predicting different clusters of ASD. Abbreviations: R TPJ, right temporoparietal junction; L Ins, left insula; L Ant IPS, left anterior intraparietal sulcus.

연세대학교
YONSEI UNIVERSITY

Table 5. Neural connectivity analysis in neuro-behavioral clusters using hub nodes

Multi-modal clusters	**Segregation**	**Hub node compensation**
Cluster 1 (good IJA)	Overall CC: 0.491	R TPJ (EC: 0.156) L Ins (EC: 0.160) L Ant IPS (EC: 0.153)
Cluster 2 (poor IJA & RJA)	Overall CC: 0.506	R TPJ (EC: 0.176) L Ins (EC: 0.156) L Ant IPS (EC: 0.154)
Cluster 3 (RJA > IJA)	Overall CC: 0.512	R TPJ (EC: 0.159) L Ins (EC: 0.155) L Ant IPS (EC: 0.162)

Abbreviations: R TPJ, right temporoparietal junction; L Ins, left insula; L Ant IPS, left anterior intraparietal sulcus.

3.2.5. Genetic profile analysis in neuro-behavioral clusters

Firstly, cluster 3 showed greatest number of total gene variants (common and rare) with 1.04×107 (8.90×106, 1.53×106). The common to rare variant ratio was highest for cluster 1 = 5.69 (0.15), indicating that the influence of common variants might be stronger than that of rare variants in this cluster. This is reflected in the higher polygenic risk scores for autism, schizophrenia in this group. The polygenic risk score of intelligence was lowest for cluster 2. These common vs. rare variant effect on the three neuro-behavioral clusters are detailed in Table 6.

Cluster 3 also displayed the highest number of rare coding variants, categorized by either CADD (0-20) or CADD (≥20). This suggests that Cluster 3 is significantly impacted by deleterious coding variants, which are likely associated with autism. Additionally, this cluster was strongly influenced by deleterious non-coding variants. In contrast, Cluster 1 showed the least influence from non-

연세대학교
YONSEI UNIVERSITY

coding variants, as it is predominantly affected by the effects of common variants. These findings are detailed in Table 7.

Table 6. Common vs. rare variants in neuro-behavioral clusters

Genetic measures	**Overall (N=31)**	**Cluster 1 (N=6)**	**Cluster 2 (N=5)**	**Cluster 3 (N=20)**
Total variants*	1.02×10^{7} (1.38×10^{6})	1.03×10^{7} (8.73×10^{4})	8.65×10^{6} (3.57×10^{6})	1.04×10^{7} (1.51×10^{5})
Common variants*	8.67×10^{6} (1.17×10^{6})	8.85×10^{6} (4.94×10^{4})	7.38×10^{6} (3.04×10^{6})	8.90×10^{6} (1.02×10^{5})
Rare variants*	1.49×10^{6} (2.11×10^{5})	1.49×10^{6} (4.27×10^{4})	1.27×10^{6} (5.37×10^{5})	1.53×10^{6} (5.59×10^{4})
Common:rare*	5.84 (0.16)	5.96 (0.15)	5.85 (0.15)	5.81 (0.16)
Autism PRS*	5.0×10^{-4} (2.0×10^{-4})	5.0×10^{-4} (1.0×10^{-4})	4.0×10^{-4} (2.0×10^{-4})	5.0×10^{-4} (2.0×10^{-4})
Schizo. PRS*	4.2×10^{-4} (8.0×10^{-5})	4.5×10^{-4} (6.0×10^{-5})	4.1×10^{-4} (6.0×10^{-5})	4.1×10^{-4} (9.0×10^{-5})
Intelligence PRS*	-6.0×10^{-5} (4.0×10^{-5})	-6.0×10^{-5} (4.0×10^{-5})	-3.0×10^{-5} (2.0×10^{-5})	-7.0×10^{-5} (4.0×10^{-5})

* Mean (SD)

Abbreviations: PRS, polygenic risk score; Schizo, schizophrenia.

연세대학교
YONSEI UNIVERSITY

Table 7. Rare variants of neuro-behavioral clusters—quantitative analysis

CADD / rare variant type	**Overall (N=31)**	**Cluster 1 (N=6)**	**Cluster 2 (N=5)**	**Cluster 3 (N=20)**
CADD (0-20) pLI > 0.9 Coding*	14.08 (11.01)	12.50 (13.00)	9.67 (7.57)	**15.11** (11.36)
CADD (≥20) pLI >0.9 Coding*	25.46 (12.52)	25.00 (6.38)	19.00 (9.85)	**26.58** (13.85)
CADD (0-20) Non-coding*	12.22 (15.99)	**9.25** (3.86)	**16.33** (17.04)	12.19 (18.09)
CADD (≥20) Non-coding*	6.48 (7.56)	**2.00** (2.16)	4.00 (0.00)	**8.06** (8.57)

* Mean (SD)

Abbreviations: CADD, combined annotation-dependent depletion; pLI, probability of being loss-of-function intolerant. pLI > 0.9: This indicates that the variants listed are in genes highly intolerant to loss-of-function mutations, with a probability greater than 90%. Such mutations in these genes are likely deleterious and contribute significantly to disease phenotypes. CADD (0-20): Variants with CADD scores in this range are considered less likely to be deleterious. These scores suggest that the genetic variants might have milder impacts on gene function and are less likely to cause harmful effects. CADD (≥20): Variants with CADD scores of 20 or above are predicted to be more deleterious. High CADD scores indicate that these variants could have significant negative impacts on gene function and are potentially associated with substantial health consequences.

3.2.5.1. Interpretation of coding genes in relation to cluster traits

To interpret the coding genes exclusive to each neuro-behavioral cluster and their associations with neurodevelopment, autism spectrum disorder (ASD), and related pathways, the specific functions and implications of these genes are examined. The qualitative analysis are shown in Table 8.

Cluster 1: good joint attention, visuospatial processing, and integration

연세대학교
YONSEI UNIVERSITY

The genes that were found exclusively in this cluster were AHDC1, HERC1, KANSL1, RALGAPB, SHANK3, ARID2, SETDB1, PLPPR4, PTPRB, PSMD11, DYNC1H1, NRXN3, CCT4, YEATS2, GRIK5, GRB10, SRCAP, and PRKD2. These genes contribute to the strong integration and efficient synaptic connectivity observed in Cluster 1, facilitating better joint attention and visuospatial processing. SHANK3 is a scaffolding protein involved in synapse formation and maintenance, crucial for the development and function of neural circuits. Mutations in SHANK3 are strongly associated with ASD and Phelan-McDermid syndrome, often leading to intellectual disability and impaired communication skills. The pathways involving SHANK3 are critical for synaptic signaling, neural connectivity, and plasticity. Mutations in AHDC1 cause Xia-Gibbs syndrome, characterized by global developmental delay and intellectual disability. This gene has been implicated in ASD due to its role in DNA repair and epigenetic regulation during neurodevelopment. GRIK5 encodes a subunit of the kainate type of glutamate receptors, important for excitatory neurotransmission in the brain. Alterations in glutamate receptors have been linked to neurodevelopmental disorders, including ASD, affecting learning and memory processes. NRXN3 is part of the neurexin family involved in synapse formation and neurotransmission. Neurexins are crucial for synaptic stability and plasticity, and mutations in these genes are associated with ASD.

Cluster 2: poor joint attention, poor integration, and overcompensated neural connectivity

The genes exclusively discovered in this cluster were: BRSK2, DLGAP3, CARD11, SETBP1, KAT2B, SMARCA4, CDKL5, SMG6, ADCY5, HDAC4, GABRB3, TSC1, MAP1B, TAOK2, TNRC6B, GRM5, CTR9, and RIMS1. The presence of these genes in Cluster 2 suggests a disruption in neural inhibition and growth pathways, contributing to poor integration and overcompensated neural connectivity observed in this cluster. GABRB3 encodes a subunit of the GABA-A receptor, which is critical for inhibitory neurotransmission in the brain. Mutations in GABRB3 have been linked to ASD, epilepsy, and Angelman syndrome, often leading to disrupted neural inhibition and balance. TSC1 is involved in the TSC1/TSC2 complex, which regulates cell growth and proliferation. Mutations in TSC1 are associated with tuberous sclerosis complex, a condition that often includes ASD and intellectual disability. CDKL5 is a serine/threonine kinase that is critical for postnatal brain development. Mutations in CDKL5 cause severe neurodevelopmental disorders, including early-onset epileptic encephalopathy with features of ASD.

연세대학교
YONSEI UNIVERSITY

Cluster 3: Mixed joint attention patterns, impaired daily living skills and motor coordination

The genes exclusively found in this cluster were: NTRK3, NFIB, ZMIZ1, CACNA1B, PTGS2, CHD8, GIGYF2, DNM1, KIAA0232, MYH9, VPS54, PRR14L, PRICKLE1, ANK3, PAK2, among others. These genes suggest that Cluster 3 may have issues related to inflammation, chromatin remodeling, and neuronal connectivity, contributing to their unique social interaction and motor coordination challenges. CHD8 is a chromodomain helicase DNA-binding protein involved in chromatin remodeling and transcriptional regulation. Mutations in CHD8 are strongly linked to ASD, often leading to macrocephaly, intellectual disability, and social interaction difficulties. The pathways involving CHD8 affect chromatin modification and gene expression critical for neurodevelopment. ANK3 encodes ankyrin-G, a protein crucial for the stability and function of neuronal axon initial segments. Variants in ANK3 have been implicated in bipolar disorder, schizophrenia, and ASD, affecting neural connectivity and signaling. PTGS2 (COX-2) encodes an enzyme involved in the inflammatory response. Inflammation has been linked to ASD, and alterations in PTGS2 expression can impact neurodevelopment and behavior.

3.2.5.2. Interpretation of non-coding genes in relation to cluster traits

To understand how the non-coding genes exclusive to certain neuro-behavioral clusters relate to neurodevelopment, autism spectrum disorder (ASD), and associated pathways, an in-depth analysis of the specific genes was conducted. The qualitative analysis are shown in Table 9.

Cluster 1: good joint attention, visuospatial processing, and integration

The genes in this cluster include SETDB1, SKI, HDLBP, CC2D1A, and DOCK8. These genes were analyzed for their functional roles and associations with ASD. These findings suggest that the genes exclusive to Cluster 1 may benefit from robust epigenetic regulation and transcriptional control, contributing to better integration and joint attention capabilities observed in individuals associated with this cluster. SETDB1 is a gene involved in the epigenetic regulation of chromatin structure, which significantly impacts gene expression. Dysregulation of SETDB1 has been linked to ASD through its critical role in neural cell differentiation and brain inflammation. Overexpression of SETDB1 is associated with neurodevelopmental abnormalities. The primary pathways influenced by SETDB1 include epigenetic regulation, chromatin modification, and neural development. SKI functions as a proto-oncogene that regulates transcription and suppresses TGF-β signaling.

연세대학교
YONSEI UNIVERSITY

Mutations or dysregulation in SKI can lead to developmental delays and congenital abnormalities that overlap with ASD features. Therefore, SKI's role in transcriptional regulation is crucial for normal neurodevelopment. High-Density Lipoprotein Binding Protein (HDLBP) is involved in RNA binding and the regulation of lipid metabolism. Although direct links to ASD are limited, disruptions in RNA binding proteins like HDLBP can affect neural development and function. The influence of HDLBP on neurodevelopment underscores its potential role in ASD-related pathways.

Cluster 2: poor joint attention, poor integration, and overcompensated neural connectivity

Cluster 2 encompasses genes that are associated with poor joint attention, poor integration, and overcompensated connectivity. The exclusive non-coding genes in this cluster include KDM4C, TAOK2, MCPH1, CSNK1G1, DMWD, SEZ6L2, NINL, KDM5A, SNX5, TAF6, DEAF1, among others. The genes in Cluster 2 highlight significant disruptions in neural development and synaptic regulation, contributing to the observed poor integration and overcompensated connectivity in affected individuals. KDM4C is a histone demethylase involved in chromatin remodeling and gene expression regulation. Dysregulation of KDM4C can disrupt normal neural development processes and has been implicated in various neurodevelopmental disorders, including ASD. The primary pathways influenced by KDM4C involve chromatin remodeling and epigenetic regulation. TAOK2 is involved in the regulation of the cytoskeleton and synaptic development. Mutations in TAOK2 have been associated with ASD and intellectual disability, influencing neural connectivity and synaptic function. This gene's role in synaptic development is critical for understanding its impact on ASD. Microcephalin 1 (MCPH1) is involved in DNA repair and cell cycle regulation. Mutations in MCPH1 can lead to primary microcephaly, characterized by a significantly smaller brain size, which can be associated with neurodevelopmental disorders including ASD. MCPH1's involvement in DNA repair pathways highlights its importance in maintaining neural integrity.

Cluster 3: Mixed joint attention patterns, impaired daily living skills and motor coordination

The genes exclusive to Cluster 3 are associated with challenges in social interaction, daily living, and motor coordination. The significant non-coding genes in this cluster include KDM6B, NRXN1, MBD1, NSD1, SRPRA, PCDHA11, SLC7A7, SAMD11, PTGS2, CHD8, among others. The genes in Cluster 3 are associated with crucial pathways in neural development, synaptic function, and epigenetic regulation. These associations help explain the unique social interaction challenges and

연세대학교
YONSEI UNIVERSITY

motor coordination issues observed in individuals related to this cluster. KDM6B is involved in histone demethylation, impacting gene expression and neural development. Mutations in KDM6B are linked to neurodevelopmental disorders, including ASD, due to their role in epigenetic regulation. The primary pathways influenced by KDM6B involve epigenetic regulation and neural development. NRXN1 is crucial for synaptic function and neural communication. Mutations in NRXN1 are strongly linked to ASD, affecting synaptic stability and plasticity. This gene's role in synaptic function is essential for understanding its contribution to ASD. CHD8 is a chromatin remodeler involved in gene transcription regulation. Mutations in CHD8 are one of the most significant genetic risk factors for ASD, impacting neurodevelopment and resulting in features such as macrocephaly and intellectual disability. CHD8's involvement in transcriptional regulation underscores its critical role in neurodevelopment.

Table 8. Rare coding variants of neuro-behavioral clusters – qualitative analysis

Variant type	**Overlapping**	**Cluster 1 (N=6)**	**Cluster 2 (N=5)**	**Cluster 3 (N=20)**
Coding	NRXN1, PLXNA4, ZNF462, MAP1A, CUX2, MYO16, KDM6B, GGNBP2, CIC, HIVEP2, WDFY4, TNRC6C, SLC12A5, SETD1B, KDM5A, SRRM2, TSHZ3, RAI1, EP400, INTS6, GABBR2, MYCBP2, UNC79, NBEA, ARNT2, RIMS2, TEK, PABPC1, MAP1B, EHMT1, JMJD1C	AHDC1, HERC1, KANSL1, RALGAPB, SHANK3, ARID2, SETDB1, PLPPR4, PTPRB, PSMD11, DYNC1H1, NRXN3, CCT4, YEATS2, GRIK5, GRB10, SRCAP, PRKD2	BRSK2, DLGAP3, CARD11, SETBP1, KAT2B, SMARCA4, **CDKL5**, SMG6, ADCY5, HDAC4, **GABRB3**, **TSC1**, MAP1B, TAOK2, TNRC6B, GRM5, CTR9, RIMS1	NTRK3, NFIB, ZMIZ1, CACNA1B, **PTGS2**, **CHD8**, GIGYF2, DNM1, KIAA0232, MYH9, VPS54, PRR14L, PRICKLE1, **ANK3**, ZNF292, ANKRD11, ADGRL1, ARHGAP5, PREX1, KMT2C, HECW2, POGZ, ASXL3, MET, SRSF1, ASH1L, CACNA1I, CLASP1, EXT1, RFX7, TBX22, PCDH19, MBD1, MYT1L, CASKIN1, CACNB1, NAV2, UBR5, BIRC6, IQSEC2, UBE3C,

연세대학교
YONSEI UNIVERSITY

	CHD3, CHD2, NCOR1, PHLPP1, SATB2, HNRNPU, ARID1B, SCAF1, SAE1, ERBIN, EMSY, SETD2, GRIN2B, GRIA1, AR, CNOT1, ANK2, KMT5B, MCM6, MYO5A, CDH8, KDM3A, TCF7L2, DST, SETD1A, CASZ1, CLIP2, DMXL2, CACNA1G, DIP2C, GRIK3, ANKRD17, TSHZ1, MAGEL2, EPC2, PTPRC, CREBBP, MAOA, CACNA1C, AGAP1, PACS1, MED12L, CHD7, KCNB1, CHD9, FGF14, PRR12, PPP3CA, NSD2, GRM7, PPFIA1, MACF1, DLGAP2, NSD1, YTHDC2, KDM4B, SCN2A, MRTFB, MYH10, FLNA, LEMD3, CACNA1A, SHANK1, PRKDC, FBN1, BTAF1, HIVEP3, RELN, SPEN, TM9SF4, SON, NR4A2, KDM3B, UBAP2L, MTOR, AUTS2, PAK2

연세대학교
YONSEI UNIVERSITY

Table 9. Rare non-coding variants of neuro-behavioral clusters – qualitative analysis

Variant type	**Overlapping**	**Cluster 1 (N=6)**	**Cluster 2 (N=5)**	**Cluster 3 (N=20)**
Non-coding	NCKAP5, CHMP1A, LILRB2, PRR12, MBOAT7, ABCA7, SLC12A5	SETDB1, SKI, HDLBP, CC2D1A, DOCK8	**KDM4C**, **TAOK2**, **MCPH1**, CSNK1G1, DMWD, SEZ6L2, NINL, KDM5A, SNX5, TAF6, DEAF1	**KDM6B**, **NRXN1**, MBD1, NSD1, SRPRA, PCDHA11, SLC7A7, SAMD11, PTGS2, **CHD8**, SMARCC2, SETD1A, DDHD2, SUPT16H, EIF4G1, CD276, PTEN, CUL7, HLA-B, SLC7A5, EXOC6B, HNRNPU, ARID1B, ANK3, PRR25, PHF12, SETD2, TM9SF4, TMEM39B, UBAP2L, TNS2, SRSF1, PRKAR1B, CLN8, MAPT-AS1, AUTS2, MUC4, DNAH10, PPFIA1, TSC2, ANK2

연세대학교
YONSEI UNIVERSITY

3.3. Multi-modal model performance

3.3.1. Autism symptom severity prediction model performance

Uni-modal vs multi-modal without retrospective cluster information vs multi-modal with retrospective cluster information. Multi-modal model showed comparable performance in autism symptom severity assessment task across all performance metrics: AUROC, accuracy, precision, and recall. The fMRI uni-modal model outperformed with respect to AUROC, and accuracy compared to that of video model. The results are presented in Table 10.

Table 10. Uni-modal vs. multi-modal model symptom severity prediction performance

Prospective dataset	AUROC	Accuracy	Precision	Recall
Video only*	0.60, 95%CI=(0.52-0.63)	0.65, 95%CI=(0.6-0.7)	0.35, 95%CI=(0.35-0.35)	0.5, 95%CI= (0.5-0.5)
rs-fMRI only*	0.86, 95%CI=(0.76,0.95)	0.7, 95%CI=(0.7,0.7)	0.35, 95%CI=(0.35-0.35)	0.5, 95%CI=(0.5-0.5)
Multi-modal (video + rs-fMRI)*	0.84, 95%CI=(0.74,0.93)	0.7, 95%CI=(0.7,0.7)	0.35, 95%CI=(0.35-0.35)	0.5, 95%CI=(0.5-0.5)
Multi-model with clustering*	0.81, 95%CI=(0.69,0.93)	0.7, 95%CI=(0.7,0.7)	0.5, 95%CI=(0.35-0.35)	0.5, 95%CI=(0.5-0.5)

* Mean (95% CI)

3.3.2. Shapley value-based visualization

Incorporating cluster information from retrospectively derived clustering algorithms into multimodal feature-based models improved the prediction of autism severity. The integration utilized a broader range of features from both modalities, rather than relying on a single modality.

연세대학교
YONSEI UNIVERSITY

This comprehensive approach is evidenced in the enhanced accuracy reflected in the Deep SHAP results, as depicted in Fig 8.

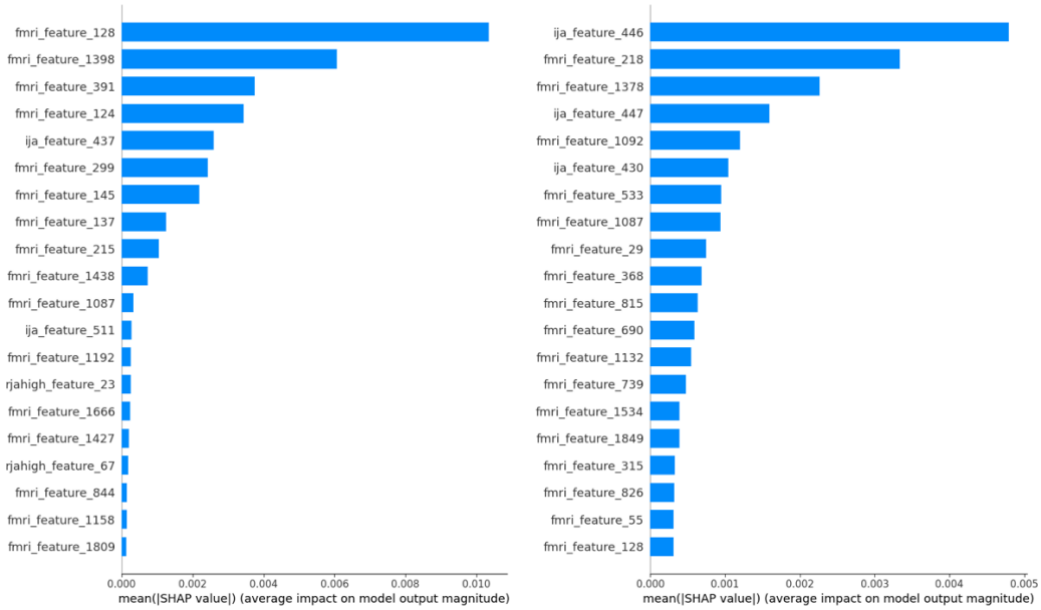

Fig 8. Multimodal features used for predicting symptom severity—Shapley values. Model prediction of autism severity using multimodal features (left) without clustering information, (right) with clustering information.

연세대학교
YONSEI UNIVERSITY

4. DISCUSSION

Our prospective study pioneers a novel approach by developing and validating a neuro-behavioral subclassification system through the concurrent collection of functional neuroimaging, neuro-behavioral video, and genomic data from the same participants, a methodology not previously attempted. The validity of these neuro-behavioral subgroups was verified through clinical presentation, gaze patterns, neural connectivity, and genetic profiles. Additionally, we evaluated the classification of autism symptom severity based on combined neural and behavioral features using supervised learning, with clinical scores as benchmarks for symptom severity, to determine if the extracted features correspond to clinically significant information. Employing meticulously designed deep learning architectures for each data type allowed us to effectively extract features. These features were then integrated and subjected to advanced clustering techniques suitable for high-dimensional data, resulting in purely data-driven neuro-behavioral clusters.

We identified three distinct neuro-behavioral clusters in individuals with autism, each comprising a mix of mild, moderate, and severe cases, as measured by the ADOS CSS—standardized scores for autism severity. Interestingly, these clusters did not differ significantly in their total ADOS CSS scores, underscoring the limitations of severity scores in forming clear, distinct groups, as noted in previous studies.[71,72] Additionally, our findings align with earlier research indicating a poor correlation between data-driven clustering and clinical severity scores.[73,74] This suggests that traditional observation-based severity assessments may not adequately capture the neuro-biological features used in unsupervised data-driven classification, such as gaze patterns or fMRI signals.

The three distinct clusters we identified in individuals with autism primarily varied based on their performance in joint attention tasks, which correlated with differences in clinical features, gaze patterns, and neural connectivity patterns. Cluster 1, characterized by mild genetic vulnerability and no significant neural connectivity abnormalities, excelled in IJA, correlating with higher IQs and milder autism symptoms. In contrast, Cluster 2 displayed pronounced impairments in joint attention tasks, coupled with hub node compensation in neural connectivity and moderate genetic vulnerability; these individuals showed profound social deficits, lower full-scale IQ, and reduced verbal comprehension, suggesting overall developmental delays. Cluster 3, which demonstrated

연세대학교
YONSEI UNIVERSITY

partial impairment in joint attention, especially in initiating tasks, exhibited the highest genetic vulnerability and marked neural segregation. This cluster also showed moderate-to-severe autistic traits and lower adaptive functioning.

Further distinguishing Cluster 2 and Cluster 3 were their distinctive substructural connectivity patterns, particularly between R TPJ—an integrative center for multimodal sensory processing—and other network regions.[75] These differences in neural connectivity support existing research suggesting that disruptions in multimodal sensory integration may underpin autism.[75,76] The variance in task performance, such as in RJA_{high} versus RJA_{low} or IJA, where RJA_{high} requires minimal effort compared to the more challenging RJA_{low} and IJA, might be attributed to the clusters' differing abilities to process sensory inputs like visual and auditory information. This aligns with the observed clinical and behavioral discrepancies across the clusters, emphasizing the value of joint attention tasks as a more effective basis for clustering than traditional severity scores.

We validated the neuro-behavioral clusters using genetic data and found differences in their genetic makeup, contributing to their distinct clinical manifestations and neural connectivity patterns. Cluster 1 had the most common variants and highest PRS for autism and schizophrenia, which are associated with milder forms of autism spectrum disorder.[77] Cluster 2 uniquely possessed SNPs related to chromatin remodeling and synaptic regulation, explaining its poor integration and overcompensated neural connectivity. This high genetic and neural burden contributed to severe social deficiency, low IQ, and overall developmental delay (language, motor, etc.). Cluster 3 had SNPs associated with key pathways in neural development, synaptic function, and epigenetic regulation. With the most influence from both coding and non-coding high-deleterious variants, in accordance with previous studies that showed association with presence of high-deleterious rare variants and increased autism severioty,[30] Cluster 3 exhibited significant difficulties in joint attention tasks, daily functioning, and fine motor control.

The explainability of our model was substantiated using Shapley values visualization. While fMRI data-driven autism symptom severity prediction was the most accurate, the multi-modal model, incorporating features from both fMRI and video, resulted in distinct clusters from genetic, neural, and behavioral perspectives. The lower prediction capacity of the video model was attributed to the

연세대학교
YONSEI UNIVERSITY

low sample size used for training via SSL. Increasing the sample size for video training would make the combined multi-modal model more robust and effective in predicting clinical traits of autism. Our preliminary results do not definitively show that a multimodal approach outperforms unimodal strategies but suggest it could extract a richer set of features relevant to autism symptom severity. In the future, with larger sample sizes, the development of such a multi-modal model could enhance feature selection and improve understanding of unique autism traits. Our clustering analysis suggests potential benefits, but further validation of the multi-modal model is needed.

Our approach holds significant potential in multimodal modeling of neurobiological conditions like ASD. By leveraging the complementary information from diverse data types, we not only deepen our understanding of individuals' autistic traits and severity but also enhance the predictive accuracy of models concerning overall symptom severity. Importantly, by integrating genetic, neural connectivity, and behavioral data from the same individuals, we can hypothesize about the constituents of their autism spectrum traits. Clinically, this enables the development of more personalized interventions, tailored to the primary challenges faced by each individual. For instance, individuals in cluster 1 could benefit more from behavioral therapies and parental guidance focused on nurturing social interactions. Conversely, for those in clusters 2 or 3, behavioral modification alone may not suffice. In such cases, genetic testing, pharmacological approaches, or neuromodulatory interventions like repetitive transcranial magnetic stimulation (r-TMS) could be necessary alternatives. Crucially, this nuanced understanding can prevent the depletion of resources on ineffective behavioral modifications when the underlying issue may be rooted more deeply in genetic or neural connectivity dysfunctions.

Strengths and limitations: The strength of our study lies in its innovative design, which collects and integrates multiple data types from a single source for clustering and classification. This approach allows for interpretations across various levels and axes, facilitating discussions about the divergent pathways within different groups—something previously unattainable in multimodal research that relied on disparate datasets. Our meticulous clustering validation, supported by visualization techniques and downstream task analysis, bolsters the credibility of the clusters identified. However, the study is constrained by the intensive nature of its design, which is highly sensitive to the patient enrollment process. Participant dropout results in the loss of multiple data points simultaneously,

연세대학교
YONSEI UNIVERSITY

complicating data collection and hindering short-term sample size expansion. Moreover, the novelty of our concept calls for replication and further studies with larger sample sizes to affirm our initial findings and extend the validity of our groundbreaking work.

5. CONCLUSION

The single-source multi-data approach utilized in this dissertation to develop a multimodal model for the subclassification of a heterogeneous disorder such as ASD has yielded promising results. The robust and reliable clustering achieved using integrated features, along with rigorous validation steps, substantiates our subclassification method. While further research involving larger cohorts or replication studies is needed to corroborate our findings, this study suggests that neuro-behavioral clustering can lead to the identification of biologically distinct groups with divergent pathways. Such insights have profound implications for advancing personalized treatment strategies that target specific issues at the genetic, neural connectivity, or behavioral levels.

연세대학교
YONSEI UNIVERSITY

REFERENCES

1. Hong SJ, Vogelstein JT, Gozzi A, et al. Toward Neurosubtypes in Autism. *Biol Psychiatry*. 2020;88(1):111-128. doi:10.1016/j.biopsych.2020.03.022
2. Cuthbert BN, Insel TR. Toward the future of psychiatric diagnosis: The seven pillars of RDoC. *BMC Med*. 2013;11(1). doi:10.1186/1741-7015-11-126
3. Insel TR. The nimh research domain criteria (rdoc) project: Precision medicine for psychiatry. *American Journal of Psychiatry*. 2014;171(4):395-397. doi:10.1176/appi.ajp.2014.14020138
4. Wolfers T, Floris DL, Dinga R, et al. From pattern classification to stratification: towards conceptualizing the heterogeneity of Autism Spectrum Disorder. *Neurosci Biobehav Rev*. 2019;104:240-254. doi:10.1016/j.neubiorev.2019.07.010
5. Lombardo M V., Lai MC, Baron-Cohen S. Big data approaches to decomposing heterogeneity across the autism spectrum. *Mol Psychiatry*. 2019;24(10):1435-1450. doi:10.1038/s41380-018-0321-0
6. Ozonoff S, Iosif AM, Baguio F, et al. *A Prospective Study of the Emergence of Early Behavioral Signs of Autism*. Vol 49.; 2010.
7. Warrier V, Zhang X, Reed P, et al. Genetic correlates of phenotypic heterogeneity in autism. *Nat Genet*. 2022;54(9):1293-1304. doi:10.1038/s41588-022-01072-5
8. Zablotsky B, Black LI, Maenner MJ, et al. Prevalence and trends of developmental disabilities among children in the United States: 2009–2017. *Pediatrics*. 2019;144(4). doi:10.1542/peds.2019-0811
9. Hodges H, Fealko C, Soares N. Autism spectrum disorder: Definition, epidemiology, causes, and clinical evaluation. *Transl Pediatr*. 2020;9:S55-S65. doi:10.21037/tp.2019.09.09
10. Kim I Bin, Lee T, Lee J, et al. Non-coding de novo mutations in chromatin interactions are implicated in autism spectrum disorder. *Mol Psychiatry*. 2022;27(11):4680-4694. doi:10.1038/s41380-022-01697-2
11. Antaki D, Guevara J, Maihofer AX, et al. A phenotypic spectrum of autism is attributable to the combined effects of rare variants, polygenic risk and sex. *Nat Genet*. 2022;54(9):1284-1292. doi:10.1038/s41588-022-01064-5
12. Hong SJ, de Wael RV, Bethlehem RAI, et al. Atypical functional connectome hierarchy in

연세대학교
YONSEI UNIVERSITY

autism. *Nat Commun*. 2019;10(1). doi:10.1038/s41467-019-08944-1

13. Choi H, Byeon K, Park B yong, et al. Diagnosis-informed connectivity subtyping discovers subgroups of autism with reproducible symptom profiles. *Neuroimage*. 2022;256. doi:10.1016/j.neuroimage.2022.119212
14. Bilder RM, Sabb FW, Cannon TD, et al. Phenomics: The systematic study of phenotypes on a genome-wide scale. *Neuroscience*. 2009;164(1):30-42. doi:10.1016/j.neuroscience.2009.01.027
15. Van Dam NT, O'Connor D, Marcelle ET, et al. Data-Driven Phenotypic Categorization for Neurobiological Analyses: Beyond DSM-5 Labels. *Biol Psychiatry*. 2017;81(6):484-494. doi:10.1016/j.biopsych.2016.06.027
16. Varoquaux G, Thirion B. *How Machine Learning Is Shaping Cognitive Neuroimaging*. Vol 3.; 2014. http://www.gigasciencejournal.com/content/3/1/28
17. Ko C, Kang S, Hong SB, et al. AI-assisted Initiation to Joint Attention Evaluation for Autism Spectrum Disorder Detection. In: *2022 IEEE 3rd International Conference on Human-Machine Systems (ICHMS)*. IEEE; 2022:1-6. doi:10.1109/ICHMS56717.2022.9980778
18. Nyström P, Thorup E, Bölte S, Falck-Ytter T. Joint Attention in Infancy and the Emergence of Autism. *Biol Psychiatry*. 2019;86(8):631-638. doi:10.1016/j.biopsych.2019.05.006
19. Mundy P, Block J, Delgado C, Pomares Y, Van Hecke AV, Parlade MV. Individual differences and the development of joint attention in infancy. *Child Dev*. 2007;78(3):938-954. doi:10.1111/j.1467-8624.2007.01042.x
20. Mundy P, Delgado C, Block J, et al. *DRAFT A Manual for the EARLY SOCIAL COMMUNICATION SCALES (ESCS)*.; 2003. http://edscholars.ucdavis.edu/vrlab/home
21. Hus V, Gotham K, Lord C. Standardizing ADOS domain scores: Separating severity of social affect and restricted and repetitive behaviors. *J Autism Dev Disord*. 2014;44(10):2400-2412. doi:10.1007/s10803-012-1719-1
22. Schaller UM, Biscaldi M, Burkhardt A, et al. ADOS-Eye-Tracking: The Archimedean Point of View and Its Absence in Autism Spectrum Conditions. *Front Psychol*. 2021;12. doi:10.3389/fpsyg.2021.584537
23. Bertelsen N, Landi I, Bethlehem RAI, et al. Imbalanced social-communicative and restricted repetitive behavior subtypes of autism spectrum disorder exhibit different neural circuitry. *Commun Biol*. 2021;4(1). doi:10.1038/s42003-021-02015-2

연세대학교
YONSEI UNIVERSITY

24. Bast N, Mason L, Ecker C, et al. Sensory salience processing moderates attenuated gazes on faces in autism spectrum disorder: a case-control study. *Mol Autism*. 2023;14(1):5. doi:10.1186/s13229-023-00537-6

25. Campbell DJ, Shic F, Macari S, Chawarska K. Gaze response to dyadic bids at 2 years related to outcomes at 3 years in autism spectrum disorders: A subtyping analysis. *J Autism Dev Disord*. 2014;44(2):431-442. doi:10.1007/s10803-013-1885-9

26. Nummenmaa L, Engell AD, Von dem Hagen E, Henson RNA, Calder AJ. Autism spectrum traits predict the neural response to eye gaze in typical individuals. *Neuroimage*. 2012;59(4):3356-3363. doi:10.1016/j.neuroimage.2011.10.075

27. Chang Z, Di Martino JM, Aiello R, et al. Computational Methods to Measure Patterns of Gaze in Toddlers with Autism Spectrum Disorder. *JAMA Pediatr*. 2021;175(8):827-836. doi:10.1001/jamapediatrics.2021.0530

28. Warrier V, Zhang X, Reed P, et al. Genetic correlates of phenotypic heterogeneity in autism. *Nat Genet*. 2022;54(9):1293-1304. doi:10.1038/s41588-022-01072-5

29. Fu JM, Satterstrom FK, Peng M, et al. Rare coding variation provides insight into the genetic architecture and phenotypic context of autism. *Nat Genet*. Published online 2022. doi:10.1038/s41588-022-01104-0

30. Choi L, An JY. Genetic architecture of autism spectrum disorder: Lessons from large-scale genomic studies. *Neurosci Biobehav Rev*. 2021;128:244-257. doi:10.1016/j.neubiorev.2021.06.028

31. Toma C. Genetic Variation across Phenotypic Severity of Autism. *Trends in Genetics*. 2020;36(4):228-231. doi:10.1016/j.tig.2020.01.005

32. Hong SJ, Valk SL, Di Martino A, Milham MP, Bernhardt BC. Multidimensional neuroanatomical subtyping of autism spectrum disorder. *Cerebral Cortex*. 2018;28(10):3578-3588. doi:10.1093/cercor/bhx229

33. Di Martino A, O'Connor D, Chen B, et al. Enhancing studies of the connectome in autism using the autism brain imaging data exchange II. *Sci Data*. 2017;4(1):170010. doi:10.1038/sdata.2017.10

34. Loth E, Charman T, Mason L, et al. The EU-AIMS Longitudinal European Autism Project (LEAP): Design and methodologies to identify and validate stratification biomarkers for autism spectrum disorders. *Mol Autism*. 2017;8(1). doi:10.1186/s13229-017-0146-8

연세대학교
YONSEI UNIVERSITY

35. Choi H, Byeon K, Park B yong, et al. Diagnosis-informed connectivity subtyping discovers subgroups of autism with reproducible symptom profiles. *Neuroimage*. 2022;256. doi:10.1016/j.neuroimage.2022.119212

36. Reardon AM, Li K, Langley J, Hu XP. Subtyping Autism Spectrum Disorder Via Joint Modeling of Clinical and Connectomic Profiles. *Brain Connect*. 2022;12(2):193-205. doi:10.1089/brain.2020.0997

37. Chen Y, Yuan J, Tian Y, et al. *Revisiting Multimodal Representation in Contrastive Learning: From Patch and Token Embeddings to Finite Discrete Tokens*.

38. Radford A, Kim JW, Hallacy C, et al. *Learning Transferable Visual Models From Natural Language Supervision*.; 2021. https://github.com/OpenAI/CLIP.

39. Ko C, Lim JH, Hong JS, Hong SB, Park YR. Development and Validation of a Joint Attention-Based Deep Learning System for Detection and Symptom Severity Assessment of Autism Spectrum Disorder. *JAMA Netw Open*. 2023;6(5):E2315174. doi:10.1001/jamanetworkopen.2023.15174

40. Heinsfeld AS, Franco AR, Craddock RC, Buchweitz A, Meneguzzi F. Identification of autism spectrum disorder using deep learning and the ABIDE dataset. *Neuroimage Clin*. 2018;17:16-23. doi:10.1016/j.nicl.2017.08.017

41. Cameron C, Yassine B, Carlton C, et al. The Neuro Bureau Preprocessing Initiative: open sharing of preprocessed neuroimaging data and derivatives. *Front Neuroinform*. 2013;7. doi:10.3389/conf.fninf.2013.09.00041

42. Cameron C, Sharad S, Brian C, et al. Towards Automated Analysis of Connectomes: The Configurable Pipeline for the Analysis of Connectomes (C-PAC). *Front Neuroinform*. 2013;7. doi:10.3389/conf.fninf.2013.09.00042

43. Varoquaux G, Gramfort A, Pedregosa F, Michel V, Thirion B. Multi-subject dictionary learning to segment an atlas of brain spontaneous activity. In: *Lecture Notes in Computer Science (Including Subseries Lecture Notes in Artificial Intelligence and Lecture Notes in Bioinformatics)*. Vol 6801 LNCS. ; 2011:562-573. doi:10.1007/978-3-642-22092-0_46

44. Chen T, Kornblith S, Norouzi M, Hinton G. *A Simple Framework for Contrastive Learning of Visual Representations*.; 2020. https://github.com/google-research/simclr.

45. Hong SJ, de Wael RV, Bethlehem RAI, et al. Atypical functional connectome hierarchy in autism. *Nat Commun*. 2019;10(1). doi:10.1038/s41467-019-08944-1

연세대학교
YONSEI UNIVERSITY

46. Khosla M, Jamison K, Ngo GH, Kuceyeski A, Sabuncu MR. Machine learning in resting-state fMRI analysis. *Magn Reson Imaging*. 2019;64:101-121. doi:10.1016/j.mri.2019.05.031

47. Liu Q, Zhang Y, Guo L, Wang ZX. Spatial-temporal data-augmentation-based functional brain network analysis for brain disorders identification. *Front Neurosci*. 2023;17. doi:10.3389/fnins.2023.1194190

48. Azevedo T, Campbell A, Romero-Garcia R, et al. A deep graph neural network architecture for modelling spatio-temporal dynamics in resting-state functional MRI data. *Med Image Anal*. 2022;79. doi:10.1016/j.media.2022.102471

49. Chen W, Shi K. Multi-scale Attention Convolutional Neural Network for time series classification. *Neural Networks*. 2021;136:126-140. doi:10.1016/j.neunet.2021.01.001

50. Sadiq A, Yahya N, Tang TB, Hashim H, Naseem I. Wavelet-Based Fractal Analysis of rs-fMRI for Classification of Alzheimer's Disease. *Sensors*. 2022;22(9). doi:10.3390/s22093102

51. Al-Hiyali MI, Yahya N, Faye I, Khan Z, Laboratoire KA. Classification of BOLD FMRI Signals using Wavelet Transform and Transfer Learning for Detection of Autism Spectrum Disorder. In: *Proceedings - 2020 IEEE EMBS Conference on Biomedical Engineering and Sciences, IECBES 2020*. Institute of Electrical and Electronics Engineers Inc.; 2021:94-98. doi:10.1109/IECBES48179.2021.9398803

52. Martínez-Vargas JD, Godino-Llorente JI, Castellanos-Dominguez G. *Time-Frequency Based Feature Selection for Discrimination of Non-Stationary Biosignals*. Vol 2012.; 2012. http://asp.eurasipjournals.com/content/2012/1/219

53. Luo FF, Wang JB, Yuan LX, et al. Higher Sensitivity and Reproducibility of Wavelet-Based Amplitude of Resting-State fMRI. *Front Neurosci*. 2020;14. doi:10.3389/fnins.2020.00224

54. Yin W, Li L, Wu FX. A Graph Attention Neural Network for Diagnosing ASD with fMRI Data. In: *Proceedings - 2021 IEEE International Conference on Bioinformatics and Biomedicine, BIBM 2021*. Institute of Electrical and Electronics Engineers Inc.; 2021:1131-1136. doi:10.1109/BIBM52615.2021.9669849

55. Chu Y, Wang G, Cao L, Qiao L, Liu M. Multi-Scale Graph Representation Learning for Autism Identification With Functional MRI. *Front Neuroinform*. 2022;15. doi:10.3389/fninf.2021.802305

연세대학교
YONSEI UNIVERSITY

56. Zhang H, Song R, Wang L, et al. Classification of Brain Disorders in rs-fMRI via Local-to-Global Graph Neural Networks. *IEEE Trans Med Imaging*. 2023;42(2):444-455. doi:10.1109/TMI.2022.3219260

57. Schanding GT, Nowell KP, Goin-Kochel RP. Utility of the Social Communication Questionnaire-Current and Social Responsiveness Scale as teacher-report screening tools for autism spectrum disorders. *J Autism Dev Disord*. 2012;42(8):1705-1716. doi:10.1007/s10803-011-1412-9

58. Frazier TW, Georgiades S, Bishop SL, Hardan AY. Behavioral and cognitive characteristics of females and males with autism in the simons simplex collection. *J Am Acad Child Adolesc Psychiatry*. 2014;53(3). doi:10.1016/j.jaac.2013.12.004

59. Park H, Seo Y, Lee J. A Study of Concurrent Validities of K-WPPSI-IV. *Korean Journal of Child Studies*. 2015;36(1):65-83. doi:10.5723/kjcs.2015.36.1.65

60. Luyster R, Gotham K, Guthrie W, et al. The autism diagnostic observation schedule - Toddler module: A new module of a standardized diagnostic measure for autism spectrum disorders. *J Autism Dev Disord*. 2009;39(9):1305-1320. doi:10.1007/s10803-009-0746-z

61. Zhang D, Li J, Shan Z. Implementation of Dlib Deep Learning Face Recognition Technology. In: *2020 International Conference on Robots & Intelligent System (ICRIS)*. IEEE; 2020:88-91. doi:10.1109/ICRIS52159.2020.00030

62. Boehm KM, Khosravi P, Vanguri R, Gao J, Shah SP. Harnessing multimodal data integration to advance precision oncology. *Nat Rev Cancer*. 2022;22(2):114-126. doi:10.1038/s41568-021-00408-3

63. Zhou T, Thung KH, Liu M, Shi F, Zhang C, Shen D. Multi-modal latent space inducing ensemble SVM classifier for early dementia diagnosis with neuroimaging data. *Med Image Anal*. 2020;60. doi:10.1016/j.media.2019.101630

64. Shwartz-Ziv R, Armon A. Tabular Data: Deep Learning is Not All You Need. Published online June 6, 2021. http://arxiv.org/abs/2106.03253

65. Wang B, Mezlini AM, Demir F, et al. Similarity network fusion for aggregating data types on a genomic scale. *Nat Methods*. 2014;11(3):333-337. doi:10.1038/nmeth.2810

66. Razavi SH, Ebadati EOM, Asadi S, Kaur H. An Efficient Grouping Genetic Algorithm for Data Clustering and Big Data Analysis. In: ; 2015:119-142. doi:10.1007/978-3-319-16598-1_5

연세대학교
YONSEI UNIVERSITY

67. Hajian-Tilaki K. Sample size estimation in diagnostic test studies of biomedical informatics. *J Biomed Inform*. 2014;48:193-204. doi:10.1016/j.jbi.2014.02.013

68. Rousseeuw PJ. Silhouettes: A graphical aid to the interpretation and validation of cluster analysis. *J Comput Appl Math*. 1987;20:53-65. doi:10.1016/0377-0427(87)90125-7

69. Davies DL, Bouldin DW. A Cluster Separation Measure. *IEEE Trans Pattern Anal Mach Intell*. 1979;PAMI-1(2):224-227. doi:10.1109/TPAMI.1979.4766909

70. von Luxburg U. A tutorial on spectral clustering. *Stat Comput*. 2007;17(4):395-416. doi:10.1007/s11222-007-9033-z

71. Mehling MH, Tassé MJ. Severity of Autism Spectrum Disorders: Current Conceptualization, and Transition to DSM-5. *J Autism Dev Disord*. 2016;46(6):2000-2016. doi:10.1007/s10803-016-2731-7

72. Cholemkery H, Medda J, Lempp T, Freitag CM. Classifying Autism Spectrum Disorders by ADI-R: Subtypes or Severity Gradient? *J Autism Dev Disord*. 2016;46(7):2327-2339. doi:10.1007/s10803-016-2760-2

73. Lombardo M V., Lai MC, Auyeung B, et al. Unsupervised data-driven stratification of mentalizing heterogeneity in autism. *Sci Rep*. 2016;6(1):35333. doi:10.1038/srep35333

74. Vandewouw MM, Brian J, Crosbie J, et al. Identifying Replicable Subgroups in Neurodevelopmental Conditions Using Resting-State Functional Magnetic Resonance Imaging Data. *JAMA Netw Open*. 2023;6(3):e232066. doi:10.1001/jamanetworkopen.2023.2066

75. Rolls ET. The cingulate cortex and limbic systems for emotion, action, and memory. *Brain Struct Funct*. 2019;224(9):3001-3018. doi:10.1007/s00429-019-01945-2

76. Kojovic, Ben Hadid, Franchini, Schaer. Sensory Processing Issues and Their Association with Social Difficulties in Children with Autism Spectrum Disorders. *J Clin Med*. 2019;8(10):1508. doi:10.3390/jcm8101508

77. Weiner DJ, Wigdor EM, Ripke S, et al. Polygenic transmission disequilibrium confirms that common and rare variation act additively to create risk for autism spectrum disorders. *Nat Genet*. 2017;49(7):978-985. doi:10.1038/ng.3863

연세대학교
YONSEI UNIVERSITY

ABSTRACT IN KOREAN

자폐스펙트럼장애의 새로운 세부 분류를 위한 뇌신경-행동학적 시스템 개발 및 검증

임상 증상의 이질성과 근본적인 신경생물학적 메커니즘은 자폐 스펙트럼 장애에 대한 개인 맞춤형 개입을 제공하는 데 상당한 어려움을 야기한다. 자폐 스펙트럼 장애의 유병률이 증가하고 사회적 영향력이 커지면서 자폐 스펙트럼 장애 표현형을 세분화하고 고유한 신경생물학적 원인을 규명하는 연구가 시급해졌다. 본 연구에서는 후향적 및 전향적 자폐스펙트럼장애 데이터를 모두 활용하여 다중모드 하위 분류 시스템을 구축하고 검증하고자 하였다. 휴지기 자기공명영상과 행동 비디오 데이터에서 추출된 특징을 통합한 다중모드 모델링은 각기 다른 임상 및 생물학적 특성을 지닌 클러스터들을 식별하는 것을 목표로 하였다.

각 데이터 유형에 맞게 정밀하게 설계된 딥러닝 아키텍처 (비디오 및 휴지기 자기공명영상)를 사용하여 주요 특징을 추출하였다. 이러한 특징을 융합한 후 고차원 데이터를 위한 고급 클러스터링 기법을 적용하여 뚜렷한 데이터 기반의 신경 행동 클러스터를 형성했다. 세개의 클러스터가 도출되었다: 특정 상황에서 유독 자폐증 관련 행동양상이 두드러지며, 유전학적 취약성이 가장 저명하고, 가장 낮은 뇌연결성을 보인 ‘클러스터 3’, 자폐증 관련 행동 패턴이 가장 두드러졌으며,

연세대학교
YONSEI UNIVERSITY

유전학적 취약성도 보이고, 저하된 뇌연결성을 특정 융합 노드가 과도한 보상을 하는 ‘클러스터 2’, 자폐증 관련 행동과 신경학적이 뚜렷하지 않으며, 일반변이의 영향을 주로 받고 희귀변이의 영향을 특히 덜 받은 ‘클러스터 1’. 융합 피쳐 추출 모델의 설명력은 샤플리 값으로 확인하고 시각화 하였다.

다중모드를 활용한 데이터 기반 중요 피쳐 추출 및 융합 방법론은 더 넓은 스펙트럼의 특징을 통해 임상적으로 뚜렷한 하위 그룹을 식별하고 자폐 증상의 심각도를 예측할 뿐만 아니라, 개별 참여자(환자)의 신경-, 행동-, 유전적- 특성을 심층적으로 이해하고, 이러한 정보가 개별 환자의 임상 표현형에 기여하는지 파악할 수 있게 하였다. 개별 환자 마다 다중 데이터를 수집하고 데이터 활용하는 연구 방법론을 도입했을 때 기대했던 결과가 초래되었으며, 통합된 특징과 철저한 검증을 통해 얻은 신뢰할 수 있는 클러스터링이 방법론이 해당 결과를 뒷받침한다. 이 연구 결과의 재현성 검증을 위해서는 대규모 또는 복제 연구가 필요하지만, 이 연구는 신경-행동 클러스터링이 고유한 경로를 가진 생물학적으로 구별되는 그룹을 식별하는 방법론으로서, 특정 유전, 신경 및 행동 문제를 타겟으로 하는 개인 맞춤형 치료 전략 수립에 기여할 수 있는 가능성을 제시한다.

핵심되는 말: 자폐스펙트럼장애, 바이오마커, 세부분류, 다중모드 데이터 융합, 딥러닝

연세대학교
YONSEI UNIVERSITY

PUBLICATION LIST

1. Ko C, Kang S, Hong SB, Park YR. Protocol for the development of joint attention-based subclassification of autism spectrum disorder and validation using multi-modal data. BMC Psychiatry. 2023;23:589. doi:10.1186/s12888-023-04978-4
2. Ko C, Lim JH, Hong J, Hong SB, Park YR. Development and Validation of a Joint Attention-Based Deep Learning System for Detection and Symptom Severity of Autism Spectrum Disorder. JAMA Netw Open. 2023;6(5):e2315174. doi:10.1001/jamanetworkopen.2023.15174
3. Ko C, Kang S, Hong SB, et al. AI-assisted Initiation to Joint Attention Evaluation for Autism Spectrum Disorder Detection. In: 2022 IEEE 3rd International Conference on Human-Machine Systems (ICHMS). IEEE; 2022:1-6. doi:10.1109/ICHMS56717.2022.9980778